Autophagy

Taylor & Francis
Taylor & Francis Group

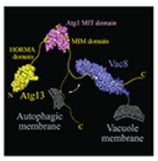

Autophagy

ISSN: (Print) (Online) Journal homepage: https://www.tandfonline.com/loi/kaup20

Induction of autophagy through CLEC4E in combination with TLR4: an innovative strategy to restrict the survival of *Mycobacterium tuberculosis*

Susanta Pahari, Shikha Negi, Mohammad Aqdas, Eusondia Arnett, Larry S. Schlesinger & Javed N Agrewala

To cite this article: Susanta Pahari, Shikha Negi, Mohammad Aqdas, Eusondia Arnett, Larry S. Schlesinger & Javed N Agrewala (2020) Induction of autophagy through CLEC4E in combination with TLR4: an innovative strategy to restrict the survival of *Mycobacterium tuberculosis*, Autophagy, 16:6, 1021-1043, DOI: 10.1080/15548627.2019.1658436

To link to this article: https://doi.org/10.1080/15548627.2019.1658436

AUTOPHAGY
2020, VOL. 16, NO. 6, 1021–1043
https://doi.org/10.1080/15548627.2019.1658436

Taylor & Francis
Taylor & Francis Group

RESEARCH PAPER

Induction of autophagy through CLEC4E in combination with TLR4: an innovative strategy to restrict the survival of *Mycobacterium tuberculosis*

Susanta Pahari[a,b], Shikha Negi[a], Mohammad Aqdas[a], Eusondia Arnett[b], Larry S. Schlesinger[b], and Javed N Agrewala[a,c]

[a]Immunology Division, CSIR-Institute of Microbial Technology, Chandigarh, India; [b]Host-Pathogen Interactions Program, Texas Biomedical Research Institute, San Antonio, TX, USA; [c]Biomedical Engineering Department, Indian Institute of Technology Ropar, Rupnagar, India

ABSTRACT

Host-directed therapies are gaining considerable impetus because of the emergence of drug-resistant strains of pathogens due to antibiotic therapy. Therefore, there is an urgent need to exploit alternative and novel strategies directed at host molecules to successfully restrict infections. The C-type lectin receptor CLEC4E and Toll-like receptor TLR4 expressed by host cells are among the first line of defense in encountering pathogens. Therefore, we exploited signaling of macrophages through CLEC4E in association with TLR4 agonists (C_4.T_4) to control the growth of *Mycobacterium tuberculosis* (*Mtb*). We observed significant improvement in host immunity and reduced bacterial load in the lungs of *Mtb*-infected mice and guinea pigs treated with C_4.T_4 agonists. Further, intracellular killing of *Mtb* was achieved with a 10-fold lower dose of isoniazid or rifampicin in conjunction with C_4.T_4 than the drugs alone. C_4.T_4 activated MYD88, PtdIns3K, STAT1 and RELA/NFKB, increased lysosome biogenesis, decreased *Il10* and *Il4* gene expression and enhanced macroautophagy/autophagy. Macrophages from autophagy-deficient (*atg5* knockout or *Becn1* knockdown) mice showed elevated survival of *Mtb*. The present findings also unveiled the novel role of CLEC4E in inducing autophagy through MYD88, which is required for control of *Mtb* growth. This study suggests a unique immunotherapeutic approach involving CLEC4E in conjunction with TLR4 to restrict the survival of *Mtb* through autophagy.

Abbreviations: 3MA: 3 methyladenine; AO: acridine orange; Atg5: autophagy related 5; AVOs: acidic vesicular organelles; BECN1: beclin 1, autophagy related; BMDMs: bone marrow derived macrophages; bw: body weight; C_4.T_4: agonists of CLEC4E (C_4/TDB) and TLR4 (T_4/ultra-pure-LPS); CFU: colony forming unit; CLEC4E/Mincle: C-type lectin domain family 4, member e; CLR: c-type lectin receptor; INH: isoniazid; LAMP1: lysosomal-associated membrane protein 1; $M\varphi^{C4.T4}$: *Mtb*-infected C_4.T_4 stimulated macrophages; MAP1LC3/LC3: microtubule-associated protein 1 light chain 3; MDC: monodansylcadaverine; MTOR: mechanistic target of rapamycin kinase; MYD88: myeloid differentiation primary response 88; NFKB: nuclear factor of kappa light polypeptide gene enhance in B cells; NLR: NOD (nucleotide-binding oligomerization domain)-like receptors; PFA: paraformaldehyde; PPD: purified protein derivative; PtdIns3K: class III phosphatidylinositol 3-kinase; RELA: v-rel reticuloendotheliosis viral oncogene homolog A (avian); RIF: rifampicin; RLR: retinoic acid-inducible gene-I-like receptors; TDB: trehalose-6,6´-dibehenate; TLR4: toll-like receptor 4; Ultra-pure-LPS: ultra-pure lipopolysaccharide-EK; V-ATPase: vacuolar-type H^+ ATPase.

ARTICLE HISTORY
Received 22 July 2018
Revised 22 July 2019
Accepted 26 July 2019

KEYWORDS
Anti-TB drugs; *atg5* knockout; autophagy; *Becn1* knockdown; CLEC4E/Mincle; host-directed immunotherapy; macrophages; *Mycobacterium tuberculosis*; TLR4; tuberculosis

Introduction

Tuberculosis (TB) is one of the top ten leading causes of death and responsible for the mortality of 1.6 million people in 2017 [1,2]. Nearly one third of the global populace is infected with *Mycobacterium tuberculosis* (*Mtb*), and 5–10% of infected individuals develop active TB [1,2]. Even though potent anti-TB drugs are available to treat the disease, their use is restricted owing to the emergence of drug resistant strains [3–5]. In addition, the lengthy treatment is associated with serious side-effects. Consequently, there is an urgent need to bring new approaches to the current regime and/or identify alternative strategies to effectively manage TB. Innovative therapies involving immunomodulators, humanized antibodies, adoptive cell therapies, host-directed remedies, etc., are being currently employed for treating cancer, autoimmunity, and cardiac diseases [6–8]. Highlighting the importance of certain immunomodulators, WHO recommends their use as adjunct therapy, along with the current TB regimen [9].

Macrophages express an array of costimulatory molecules, and different pattern recognition receptors (PRRs) [10]. During infection, recognition of pathogen-associated molecular patterns (PAMPs) through these molecules can activate macrophages [10]. CLEC4E (c-type lectin domain family 4, member e) is a PRR that contributes to the recognition of *Mtb* and enhances adaptive immune responses [11]. Mice deficient in *clec4e*$^{-/-}$ show impaired cytokine release by *Mtb*-infected macrophages [11]. The first CLEC4E ligand identified was a nucleo-protein, SAP130, which is involved in responses to stroke and traumatic brain injury [12–14]. Furthermore, macrophages expressing CLEC4E can recognize *Candida albicans* [15–17], Malassezia

CONTACT Javed N Agrewala jagrewala@iitrpr.ac.in Immunology Laboratory, CSIR-Institute of Microbial Technology, Chandigarh 160036, India
Supplemental data for this article can be accessed here.

spp [18,19], and *Fonsecaea monophora* [20]. Consequently, CLEC4E contributes to the release of pro-inflammatory cytokines and protective immune responses.

The mycobacterial cord factor trehalose-6,6′-dimycolate (TDM) is an important virulence factor of *Mtb*. In addition, it has adjuvant properties and causes inflammatory response [21,22]. The synthetic analogue of TDM is trehalose-6,6′-dibehenate (TDB), which is the active constituent of TB vaccine CAF01 that has entered into phase I clinical trials [23,24]. TDB is non-toxic, safe and induces strong cell mediated and humoral immunity [25–27], and is an agonist for CLEC4E.

Further, toll-like receptors (TLRs) play a crucial function in macrophage maturation and activation [28,29]. Even though innate immune responses against *Mtb* can signal *via* TLR2, 4 and 9, their role appears to be limited and requires extensive investigation to be fully elucidated [30]. Recently, the Food and Drug Administration (FDA) approved a TLR4 agonist (mono phosphoryl lipid A/LPS) for human therapy [31]. The optimum dose of LPS does not induce adverse effects [32,33]. C-type lectin receptors (CLRs) in conjunction with TLRs further bolster the immune response [34,35].

The role of autophagy in protection against *Mtb* is well-known [36–39]. Autophagy targets antigens for lysosomal degradation and transports microbial peptides for MHC presentation [38,39]. At the same time, it increases cell survival by inhibiting inflammatory responses [37]. TLR4 is a strong activator of autophagy [40,41]. In the current study, we are reporting an interesting and novel role for CLEC4E in inducing autophagy against *Mtb* infection. We activated *Mtb* infected macrophages by stimulating the cells with CLEC4E and TLR4 (denoted as $C_4.T_4$) agonists TDB and ultra-pure-LPS, respectively, and noted significant augmentation in the bactericidal activity of macrophages. Of key importance, macrophages from *Becn1/Beclin1* knockdown and *atg5* knockout (*atg5*$^{fl/fl}$*-Lyz2/LysM-Cre*) mice exhibited increased survival of *Mtb* even when treated with $C_4.T_4$. The mechanism uncovered in $C_4.T_4$-induced killing of *Mtb* by macrophages was through MYD88-mediated activation of the class III phosphatidylinositol 3-kinase (PtdIns3K) pathway, which led to the induction of autophagy. In the future, immunotherapy involving $C_4.T_4$ agonists may serve as an alternative strategy to treat TB patients.

Results

Signaling through CLEC4E and TLR4 enhanced macrophage activation

Macrophage activation is crucial in combating pathogens [42] and can be assessed by morphology, expression of costimulatory molecules, cytokine release and antigen processing and presentation. We monitored whether stimulation of macrophages using CLEC4E and TLR4 agonists ($C_4.T_4$) could enhance their ability to activate T cells. Interestingly, we observed that bone marrow derived macrophages (BMDMs) triggered by $C_4.T_4$, exhibited an activation phenotype, as evidenced by increased size and granularity, as depicted by scanning electron microscopy (SEM), and significantly ($p < 0.001$) improved secretion of nitric oxide (NO), as compared to unstimulated control or controls stimulated with either C_4 or T_4 (Figure 1A,B). Next, we were curious about the specificity of the signals provided through CLEC4E and TLR4 in the activation of macrophages. CLEC4E signaling regulates through SYK (spleen tyrosine kinase) [43,44]. Therefore, the activities of CLEC4E and TLR4 were blocked using their inhibitors piceatannol and CLI-095, respectively. A significant ($p < 0.001$) reduction in the release of NO and IL6 was observed in cell cultures with the inhibitors. Therefore, these data confirmed the specificity of CLEC4E and TLR4 signaling (Figure 1B,C). Next, titration was performed to identify the optimum dose of $C_4.T_4$ agonists. CLEC4E and TLR4 agonists led to the optimum release of IL6 at 24 μg/ml and 10 ng/ml, respectively. Further, these concentrations showed no effect on the viability of macrophages (Figures S1 and S2). These concentrations were chosen for all subsequent experiments. We observed homogeneous expression of CLEC4E and TLR4 on the macrophages by fluorescence microscopy and flow cytometry (Figure S3A–C). We noticed that the expression of CLEC4E and TLR4 was upregulated on *Mtb*-infected macrophages (Figure S3D,E).

The release of pro-inflammatory cytokines contributes to protection against *Mtb* [45]. We observed a significant increase in the release of IL6 ($p < 0.0001$), IL12B ($p < 0.001$), TNF ($p < 0.001$), and IL1B ($p < 0.01$) upon stimulation of *Mtb*-infected macrophages with $C_4.T_4$ combinatorial therapy ($M\varphi^{C4.T4}$) (Figure 1D–G). In contrast, a decrease in the level of IL10 ($p < 0.01$) was noted (Figure 1H). The increased levels of *Il6* ($p < 0.001$), *Il12b* ($p < 0.05$) and *Il1b* ($p < 0.01$) was further verified by RT-qPCR (Figure S4A–C).

For optimum T cell activation, two signals are essential; occupancy of TCRs by peptide-MHC complexes and subsequent activation of costimulatory molecules. Without the activation of costimulatory molecules, T cells undergo anergy [45]. Here, we observed up-regulated expression of costimulatory molecules CD40, CD86, and H2/MHC-II (histocompatibility 2) on $M\varphi^{C4.T4}$. These result suggested that $M\varphi^{C4.T4}$ attain augmented capacity to activate T cells (Figures 1I–K and S4D–F).

Triggering with $C_4.T_4$ enhanced antigen uptake potency of macrophages

Macrophages are highly potent phagocytic cells [46–49]. $M\varphi^{C4.T4}$ increased uptake of GFP-H37Ra, as demonstrated by confocal microscopy and flow cytometry (Figures 1L,M and S5). Further, these results were corroborated with CFU assays ($p < 0.01$) with H37Rv (Figure 1N). These experiments indicated that combinatorial signaling upon stimulation with $C_4.T_4$ agonists boosted the macrophage potential to phagocytose *Mtb*.

CLEC4E and TLR4 agonists enhanced macrophage bactericidal activity

Based on the increased phagocytic activity, we subsequently analyzed the bactericidal activity of the $M\varphi^{C4.T4}$. Mφ were first infected with *Mtb*, followed by stimulation through $C_4.T_4$ for 48 h. Further, to establish the specificity of the CLEC4E and TLR4 signaling, we used their inhibitors (piceatannol, SYK inhibitor) and CLI-095, respectively, and enumerated *Mtb* killing by CFU. As compared to unstimulated macrophages, $M\varphi^{C4.T4}$ showed enhanced bactericidal activity, as evidenced by significant reduction ($p < 0.0001$) in CFUs (Figure 2). Intriguingly, we noticed a significant ($p < 0.01$) increase in the survival of *Mtb* in the $M\varphi^{C4.T4}$ when signaling

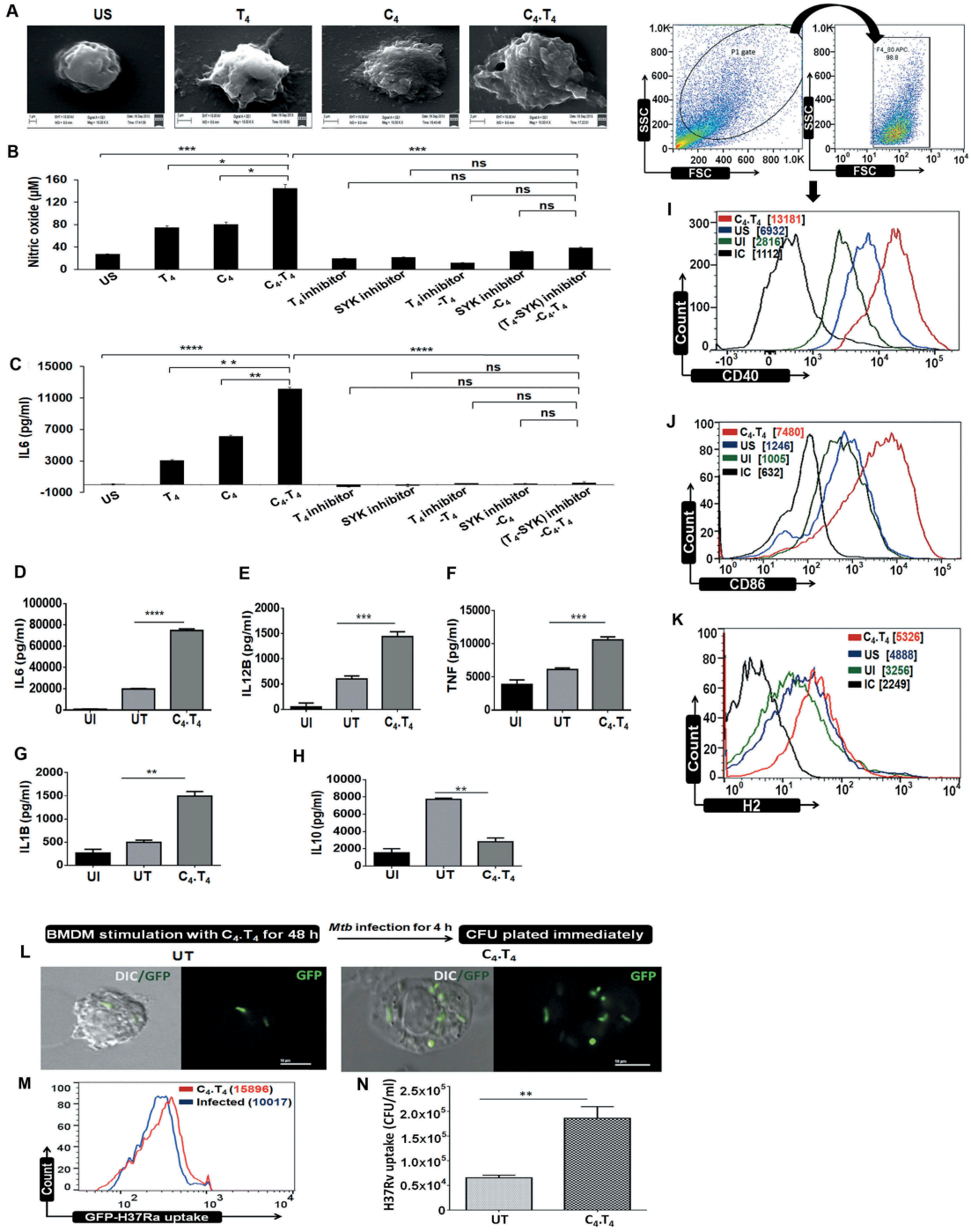

Figure 1. CLEC4E and TLR4 signaling induced the activation and maturation of macrophages. BMDMs were stimulated with the agonists of CLEC4E (C_4 [24 μg/ml]) and TLR4 (T_4 [10 ng/ml]) individually or in combination ($C_4.T_4$) for 48 h. (A) The cells were placed on glass coverslips and fixed with modified Karnoyses fixative and processed for scanning electron microscopy (SEM). Scale bar: 2 μm; magnification: 15000X. Data are representative of 2 independent experiments. (B,C) BMDMs were treated with CLEC4E (SYK-piceatannol) and TLR4 (CLI-095) signaling inhibitors for 1 h prior to $C_4.T_4$ stimulation, and then SNs were collected. The specificity of signaling was established through NO and IL6 release. (D–K) BMDMs were infected with *Mtb* for 4 h, treated with $C_4.T_4$ for 48 h and SNs were collected for the estimation of (D) IL6; (E) IL12B; (F) TNF, (G) IL1B, and (H) IL10 by ELISA. Data represent the mean ± SEM of 4 wells and are from 3 independent experiments. Further, the cells were evaluated for the expression of (I) CD40; (J) CD86; and (K) H2/MHC-II on ADGRE1/F4/80 gated cell populations by flow cytometry. All pooled MFI values from all replicates have been added to Figure S4D-F. Data represent the mean ± SEM of 2 wells and are from 2–3 independent experiments. (L–N) BMDMs were stimulated with the ligand of CLEC4E (C_4 [24 μg/ml]) and TLR4 (T_4 [10 ng/ml]) for 48 h. The cells were infected with GFP-H37Ra and phagocytosis was analyzed by (L) confocal microscopy (DIC and GFP); (M) flow cytometry. Scale bar: 10 μm. Data in each histogram overlay depicted the MFI, which was shown as bar diagram in Figure S4. (N) BMDMs were stimulated with $C_4.T_4$ for 48 h, followed by infection with H37Rv and phagocytosis was validated by CFU after 4 h. Data represents the mean ± SEM of 4 wells and are from 2–3 independent experiments. (A–N) IC, isotype control; US, unstimulated; UI, uninfected; UT, untreated and infected; C_4, CLEC4E agonist (TDB); T_4, TLR4 agonist (ultra-pure LPS); ns, non-significant. Data were analyzed by one-way ANOVA repeated measure *p ≤ 0.05, **p ≤ 0.01, ***p ≤ 0.001, ****p ≤ 0.0001.

through CLEC4E and TLR4 was blocked (Figure 2A). These experiments confirmed the specificity of $C_4.T_4$ in signaling through CLEC4E and TLR4 to regulate macrophage function. Further, we validated our results with the attenuated *Mtb*-H37Ra strain ($p < 0.01$) and *M. smegmatis* ($p < 0.001$) (Figure S6A,B).

Next, we investigated whether activating macrophages with $C_4.T_4$ could potentiate the efficacy of rifampicin (RIF) and isoniazid

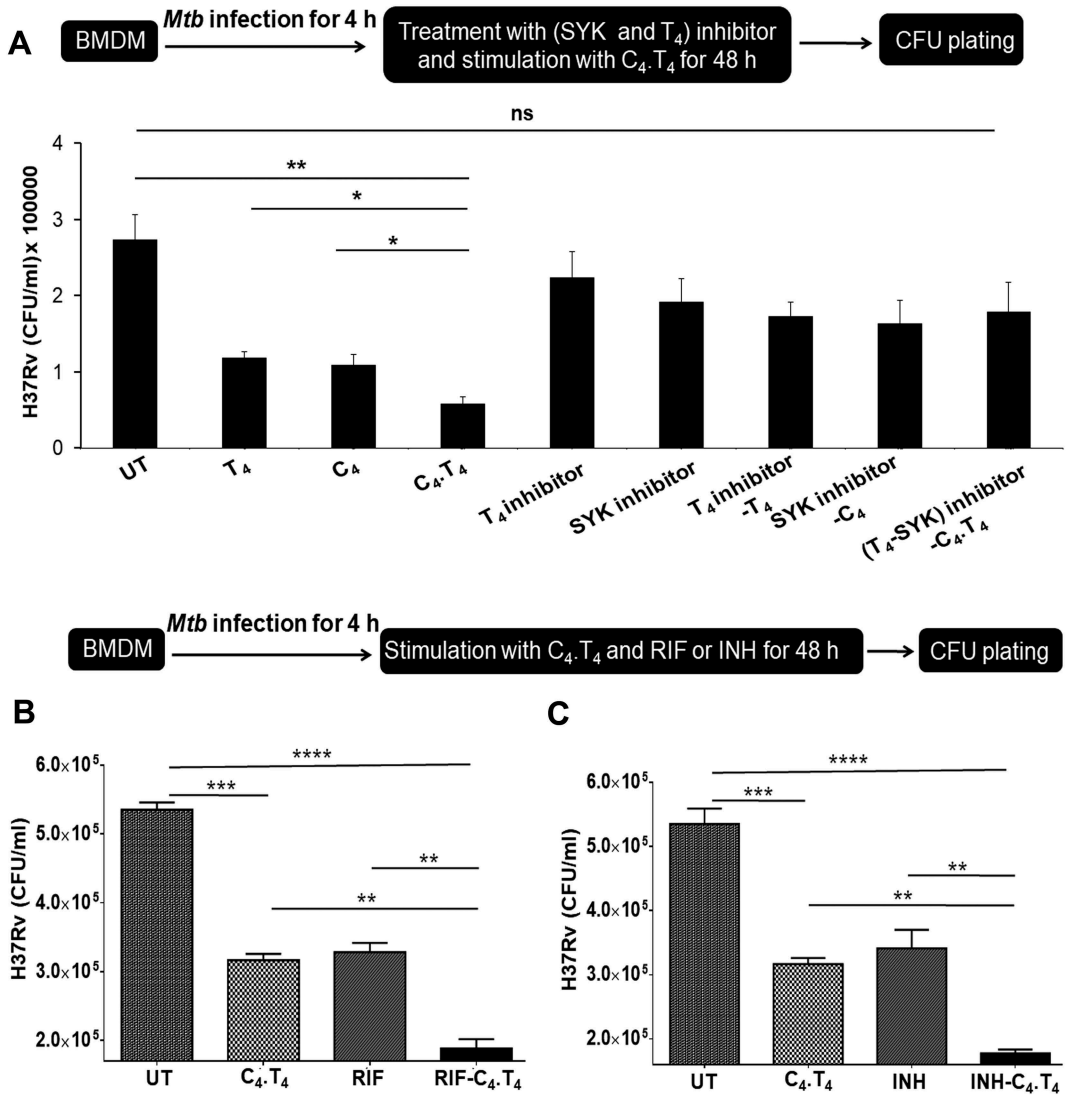

Figure 2. Adjunct therapy with $C_4.T_4$ in combination with anti-TB drugs restricted the survival of *Mtb*. (A) BMDMs were infected with H37Rv for 4 h and treated with CLEC4E (SYK-piceatannol) and TLR4 (CLI-095) signaling inhibitors for 1 h, prior to $C_4.T_4$ stimulation for 48 h, then (B,C) infected cells were treated with (B) rifampicin (0.5 µg/ml) or (C) isoniazid (2.5 µg/ml) along with $C_4.T_4$ for 48 h. The infected macrophages were lysed and CFUs were enumerated after 21 d. UT, untreated and *Mtb* infected; C_4, CLEC4E agonist (TDB); T_4, TLR4 agonist (ultra-pure LPS); ns, non-significant; RIF, rifampicin; INH, isoniazid. Data present as the mean ± SEM of 4 wells and are from 3 independent experiments. Data were analyzed by one-way ANOVA repeated measure *p ≤ 0.05, **p ≤ 0.01, ***p ≤ 0.001, ****p ≤ 0.0001.

(INH) to kill *Mtb*. We noted a significant enhancement in the efficacy of RIF ($p < 0.01$) and INH ($p < 0.01$) to kill *Mtb* in $M\varphi^{C4.T4,}$ as compared to the drugs alone (Figure 2B,C). These results suggested that adjunct therapy involving the agonists $C_4.T_4$ along with RIF and INH would improve the efficacy of anti-TB drugs, at a substantially lower drug dose than that of the currently used regimen.

Treatment with the agonists $C_4.T_4$ restricted the growth of Mtb *and improved the potency of drugs in the murine and guinea pig models of TB*

We next assessed *in vivo* efficacy of the agonists $C_4.T_4$. Administration of $C_4.T_4$ to *Mtb*-challenged mice protected them, as indicated by a statistically significant decline in bacterial burden in the lungs ($p < 0.0001$), liver ($p < 0.0001$) and spleen ($p < 0.0001$), as compared to the PBS (placebo) group (Figure 3A). Further, $C_4.T_4$ treatment substantially decreased the number ($p < 0.001$) of granulomas in the lung, as evidenced by lung morphology and granulomatous lesions, and perivascular and peribronchiolar cuffing in histopathological samples. We noted that granulomas were less consolidated with more normal alveolar structures in $C_4.T_4$-immunized lungs. More infiltration and accumulation of lymphocytes were observed in the non-immunized placebo control mice (Figure 3B,C). Next, we investigated whether treatment with $C_4.T_4$ agonists potentiate the efficacy of anti-TB drugs even at a lower dose than the recommended concentration [50]. Interestingly, we observed that treatment of mice with $C_4.T_4$ in combination with RIF considerably ($p < 0.001$) boosted the killing efficacy of the drug, when compared to the drug alone (Figure 3D). It is important to note that 1 mg/kg body weight (bw) of RIF in combination with $C_4.T_4$ decreased *Mtb* CFUs more than 10 mg/kg bw of RIF alone. Furthermore, improved killing efficacy of *Mtb* was achieved with only 2 oral doses (1 mg/kg bw) in combination

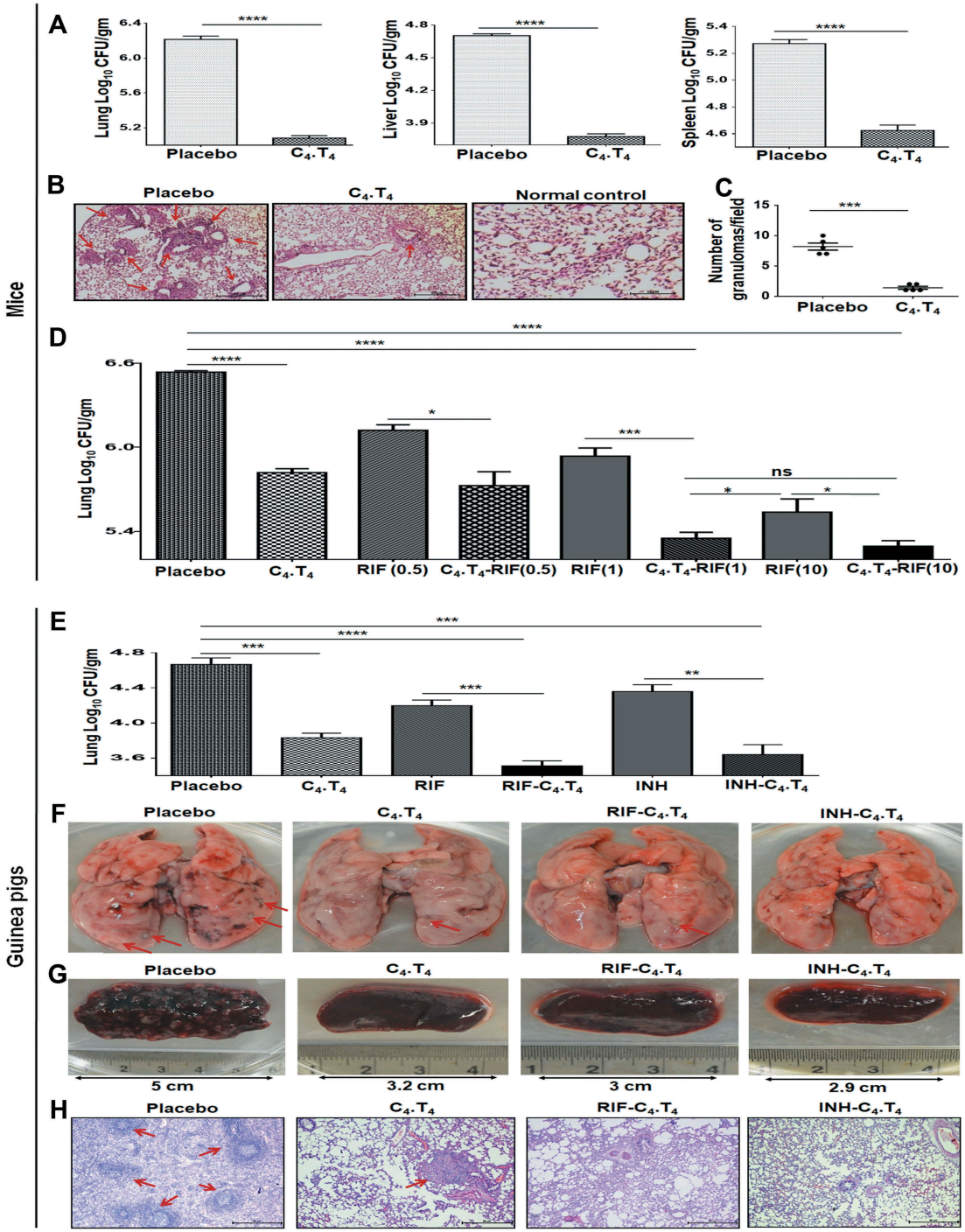

Figure 3. $C_4.T_4$ improved the efficacy and reduced the dose of anti-TB drugs in mice and guinea pigs. (A–D) *Mtb*-infected mice were treated with $C_4.T_4$. After 45 d, mycobacterial load in the (A) lungs, liver and spleen were enumerated by CFU plating. (B) Photomicrographs (10X) of H & E stained lung sections; (C) the number of granulomas/field. Scale bar: 50 µm. (D) *Mtb*-infected mice were administered $C_4.T_4$ in combination with anti-TB drugs (RIF: 0.5 mg, 1 mg and 10 mg/kg bw). After 45 d, mycobacterial load in the lungs was enumerated by CFU plating. Data represent CFU/gm wt of lungs. Control group was injected with only PBS (placebo). Data are mean ± SEM from 3 independent experiments (n = 4 mice/group). Data were analyzed by one-way ANOVA repeated measure *p ≤ 0.05, ***p ≤ 0.001, ****p ≤ 0.0001. (E–H) Guinea pigs infected with *Mtb* were treated with the $C_4.T_4$ along with anti-TB drugs (RIF: 6 mg/kg bw; INH: 5 mg/kg bw). After 45 d, (E) *Mtb* load in the lungs was enumerated by CFU plating. Data represent CFU/gm wt of lungs. Gross pathology photomicrograph showed granulomas in the (F) lungs and (G) spleen (n = 4 animals/group). Size of the spleen is indicated by the scale bar. (H) Photomicrographs (10X) of H & E stained lung sections. Scale bar: 50 µm. Control group of guinea pigs was administered only PBS (placebo). Red arrows indicated the granulomas. Normal, animals not exposed with *Mtb*; Placebo, animals exposed to *Mtb*; $C_4.T_4$, *Mtb*-exposed animals treated with $C_4.T_4$; RIF, rifampicin; INH, isoniazid. Data (mean ± SEM) are from 2 independent experiments (n = 3 guinea pigs/group unless otherwise indicated). Data were analyzed by one-way ANOVA repeated measure **p ≤ 0.01, ***p ≤ 0.001, ****p ≤ 0.0001.

with $C_4.T_4$, as compared to the recommended daily drug regime (Figure 3D).

The guinea pig model of TB is a gold standard for validating the efficacy of murine results. We observed that treatment with $C_4.T_4$ significantly ($p < 0.001$) decreased *Mtb* burden in guinea pig lungs (Figure 3E), and substantially increased the killing efficacy of RIF ($p < 0.001$) and INH ($p < 0.01$), as illustrated by decreased lung CFUs. Gross pathology of the

lungs and spleen suggested nearly normal morphology of animals injected with $C_4.T_4$, as compared to placebo control. Improved lung and spleen architecture were also observed (Figure 3F,G). The lungs were less consolidated with more normal alveolar structures in $C_4.T_4$-immunized animals, which was further improved in the groups that received $C_4.T_4$ with RIF or INH (Figure 3H). These results indicated the *in vivo* efficacy of $C_4.T_4$ in confining the growth of *Mtb* in both murine and guinea pig models.

Treatment of mice with $C_4.T_4$ expanded the pool of Th1 cells and Th17 cells against Mtb

Next, we administered $C_4.T_4$ to the *Mtb*-challenged mice. The animals were sacrificed, and splenocytes were cultured *in vitro* with PPD to assess *Mtb*-specific T cell responses. In splenocytes from $C_4.T_4$ treated mice, *Mtb*-reactive CD4 T cells ($p < 0.0001$) and CD8A T cells ($p < 0.01$) proliferated significantly more than those isolated from the placebo (PBS) control (Figure 4A–D). Likewise, significantly ($p < 0.001$) greater proliferation of T cells was noticed in the case of splenocytes isolated from $C_4.T_4$-treated guinea pigs (Figure 4E,F). These results demonstrated that signaling of macrophages through $C_4.T_4$ improved the activation of *Mtb*-specific T cells.

Besides Th1 cells, Th17 cells are also crucial for protection against *Mtb* [51,52]. We noted Th1 cells and Th17 cells expansion in the animals that were given $C_4.T_4$, as indicated by significantly higher production of IFNG ($p < 0.01$) and IL17A ($p < 0.001$) by CD4-positive T cells that had been isolated from the lungs and *in vitro* stimulated with PPD (Figures 4G–J and S7). Similarly, significantly increased expression of IFNG ($p < 0.05$) and IL17A ($p < 0.001$) was observed in CD8A-positive T cells (Figure S8A–D). Furthermore, we observed notable proliferation of T cells gated on either CD4-IFNG ($p < 0.001$) or CD4-IL17A ($p < 0.001$) (Figure 4K–N).

Polyfunctional T cells produce multiple cytokines and are thought to function better at protection against *Mtb* than their counterparts that secrete only single cytokines [53–55]. The cells isolated from the mice injected with $C_4.T_4$ showed a higher frequency of $IFNG^+$-TNF^+ ($p < 0.01$) and $IL17A^+$-TNF^+ ($p < 0.01$) polyfunctional CD4 T cells, as compared to placebo control (Figure 4O–R). Secretion of IFNG in combination with TNF by T cells has direct correlation with protection against *Mtb* by promoting the induction of autophagy [56]. Further, IL17A imparts protection by chemokine-mediated recruitment of Th1 cells at the site of infection [57].

We also demonstrated the role of $M\varphi^{C4.T4}$ in stimulating T cells *in vitro*. CD4-positive T cells were isolated from *Mtb*-challenged mice and the macrophages were derived from BMDMs. CD4-positive T cells were carboxyfluorescein diacetate N-succinimidyl ester (CFSE)-labeled and co-cultured with *Mtb*-infected $M\varphi^{C4.T4}$. We observed increased T cell proliferation with $M\varphi^{C4.T4}$, compared to control Mφ (Figure S9A). Our data suggested the immunomodulatory potential of $C_4.T_4$ bolstered both *in vivo* and *in vitro* immunity against *Mtb*.

Treatment of mice with $C_4.T_4$ generated memory CD4 T cells

Mice were challenged with *Mtb* and then administered $C_4.T_4$. The animals were sacrificed, and lung cells were isolated to monitor memory CD4-positive T cells. As expected, *Mtb* infection increased the percentage of central memory ($CD44^{hi}$-$SELL/CD62L^{hi}$) ($p < 0.0001$) and effector memory ($CD44^{hi}$-$SELL/CD62L^{lo}$) ($p < 0.01$) CD4 T cells, and these populations were further increased in the group treated with $C_4.T_4$ (Figures 5A–C and S10). Further, we observed a significant ($p < 0.001$) increase in the frequency of memory cells ($CD4^+$-$IL7R/CD127^{hi}$); thereby confirming the above data (Figure 5D). We further confirmed our results by observing an enhanced level of memory CD4 T cells ($CD4^+$-$CD44^{hi}$-$SELL/CD62L^{hi}$) *in vitro* by co-culturing CD4-positive T cells isolated from *Mtb*-challenged mice with *Mtb*-infected $M\varphi^{C4.T4}$ (Figure S9B). Activated APCs capture antigen from the infection site and then migrate towards the draining lymph nodes to activate naive T cells. CCR7 is responsible for the migration of APCs [58,59]. We observed a significantly larger ($p < 0.0001$) population of $CD44^+$-$CCR7^{hi}$ expressing T cells in *Mtb*-infected animals that received $C_4.T_4$ (Figure 5E). Overall, these data suggest that $C_4.T_4$ therapy enhanced the immunological memory and migratory potential of CD4 T cells.

Treatment of mice with $C_4.T_4$ enhanced autophagy gene expression

Autophagy has been suggested to play an important role in protection against *Mtb* [47,60,61]. Consequently, we next wanted to monitor autophagy in the *Mtb*-challenged mice that were treated with $C_4.T_4$. Interestingly, the lung cells of these animals showed a substantial reduction in *Mtb* burden (Figure 3D) and a significant increase in the expression of the autophagy genes *Atg5* ($p < 0.0001$), *Atg7* ($p < 0.0001$), *Lc3* ($p < 0.01$), *Becn1* ($p < 0.0001$), *Atg12* ($p < 0.001$), *Lamp1* ($p < 0.0001$), and *Eea1* ($p < 0.01$) (Figure 6A–G). Further, reduced *Il4* ($p < 0.0001$) and *Il10* ($p < 0.01$) gene expression was noted (Figure 6H–I). *Il4* and *Il10* genes are known to inhibit autophagy [56,62,63]. These results indicated a correlation between increased autophagy gene expression and reduced *Mtb* growth after $C_4.T_4$ treatment of mice.

$C_4.T_4$ enhanced autophagy flux through MYD88-mediated, MTOR-independent activation of PtdIns3K

We next determined if the *in vivo* findings of $C_4.T_4$ induced autophagy gene expression correlates with autophagy activation in macrophages. The conversion of LC3-I to LC3-II is one of the fundamental indicators of autophagy [47,61,64,65]. We observed conversion of LC3-I to LC3-II in $C_4.T_4$-stimulated, *Mtb*-infected macrophages (Figure 7A). This finding demonstrated the novel role for CLEC4E in inducing autophagy. We measured autophagic flux by probing for SQSTM1/p62 degradation and inhibited this with bafilomycin A_1. Bafilomycin A_1 prevents activation and maturation of autophagic vacuoles by impeding vacuolar-type

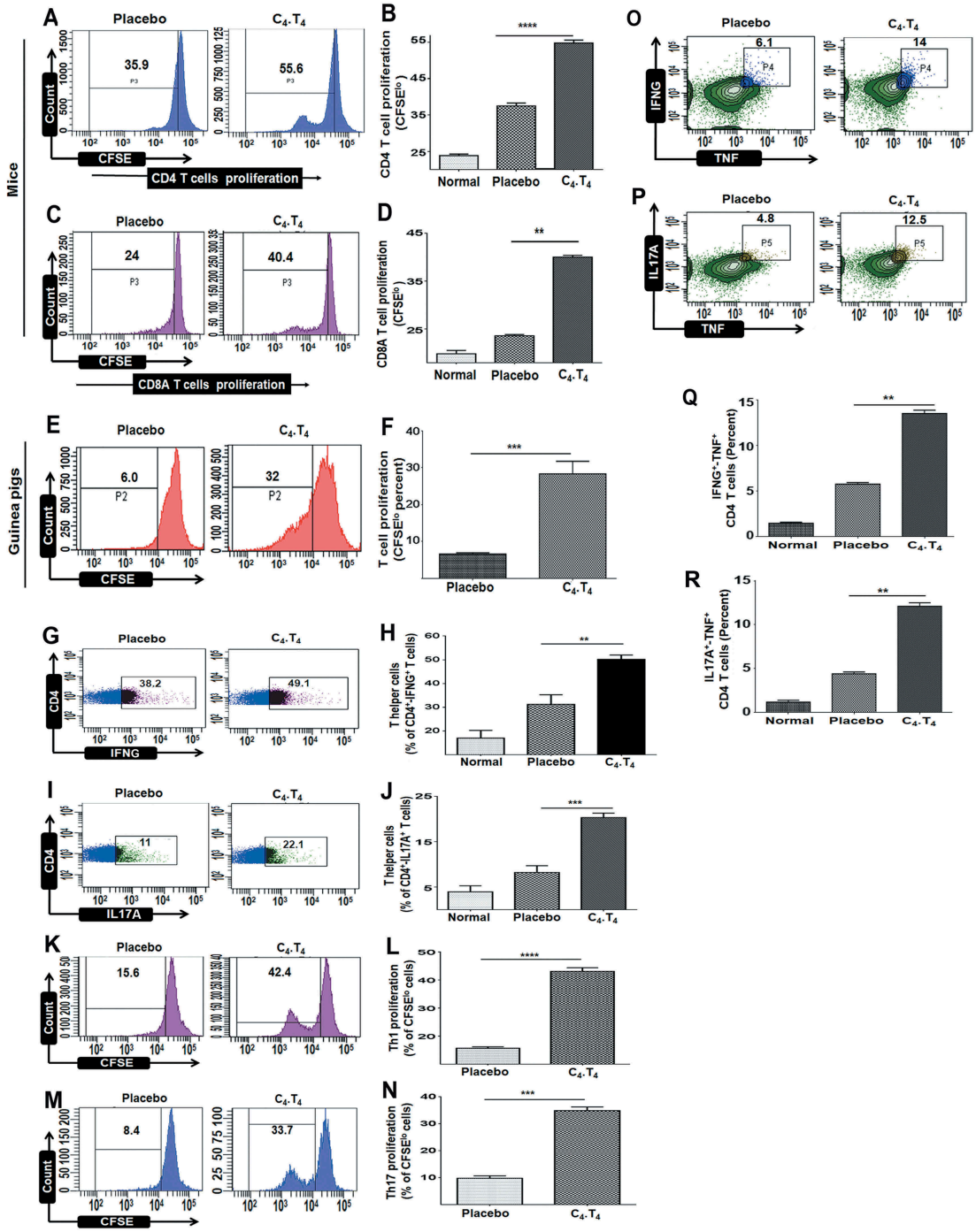

Figure 4. Treatment with $C_4.T_4$ augmented the proliferation of T cells and evoked Th1 and Th17 immune responses in *Mtb*-infected mice and guinea pigs. *Mtb*-challenged animals were treated with $C_4.T_4$. After 45 d, splenocytes were isolated and CFSE labeled. Proliferation of (A,B) CD4 T cells and (C,D) CD8A T cells was examined. (E,F) T cell proliferation of cells isolated from the spleen of guinea pigs. Data in the inset of flow cytometer histograms depicted percentage of $CFSE^{lo}$ cells and were correspondingly shown as bar diagrams (B,D,F). Intracellular staining of (G,H) $IFNG^+$ and (I,J) $IL17A^+$ was measured by flow cytometry in CD4 T cells isolated from the lung. The CD4 gated T cells showed intracellular expression of (K,L) IFNG and (M,N) IL17A were examined for proliferation through CFSE-dye dilution assay. The number in the inset of the flow cytometry plots depicted percentage of cells (G,I,K,M). Bar diagrams show pooled data from 2–3 independent experiments (H,J,L, N). (O–R) The cells isolated from lungs were stimulated with $C_4.T_4$ for 72 h and intracellular staining was done for (O,Q) IFNG-TNF, (P,R) and IL17A-TNF in CD4 gated polyfunctional T cells. Numbers in the inset of the flow cytometry plots depicted the percentage of cells. The flow cytometry data are also shown as bar diagrams and are pooled data from 2–3 independent experiments (Q,R). Normal, animals not exposed to *Mtb*; Placebo, animals exposed to *Mtb*; $C_4.T_4$, *Mtb*-exposed animals treated with $C_4.T_4$. Data are mean ± SEM from 2–3 independent experiments (n = 4 mice/group), each performed in triplicate. Data were analyzed by one-way ANOVA repeated measure **p ≤ 0.01, ***p ≤ 0.001, ****p ≤ 0.0001.

H^+ ATPase (V-ATPase), thus avoiding degradation of autophagosomes [66,67]. Interestingly, we observed a substantial decrease in SQSTM1 expression in $C_4.T_4$-stimulated macrophages (Figure 7B) and expression of SQSTM1 was induced by bafilomycin A_1 treatment in *Mtb*-infected macrophages. This observation suggested that the augmented conversion to LC3-II by $C_4.T_4$ was due to increased autophagic flux. In addition, $C_4.T_4$ induced autophagy in macrophages infected with either virulent (H37Rv) or avirulent (H37Ra) strains of *Mtb* (Figure S11A,B). We also observed increased LC3 puncta formation, as visualized using

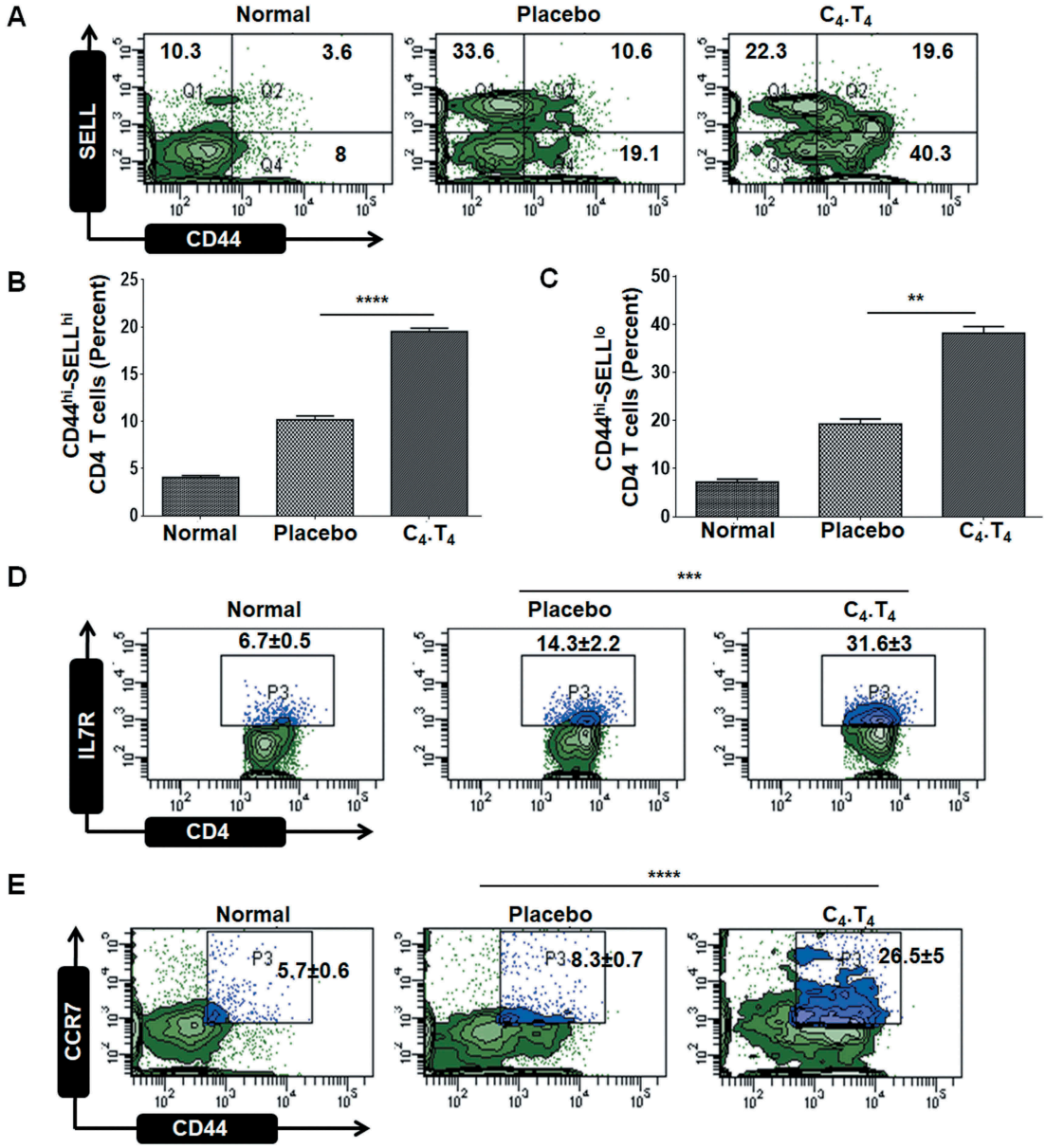

Figure 5. Signaling through CLEC4E and TLR4 generated sustained memory CD4 T cells. Mice were challenged with *Mtb* and treated with $C_4.T_4$. The control group was administered PBS (placebo). After 45 d, cells were isolated from the lungs, *in vitro* cultured with PPD for 48 h and analyzed for the expression of (A,B) central memory ($CD4^+$-$CD44^{hi}$-SELL/$CD62L^{hi}$); (A,C) effector memory ($CD4^+$-$CD44^{hi}$-SELL/$CD62L^{lo}$); (D) $CD4^+$-IL7R/$CD127^{hi}$; (E) $CD4^+$-$CD44^+$-$CCR7^{hi}$ markers by flow cytometry. The number in the inset of the flow cytometry dot plots depicted the percentage of cells. Normal, animals not exposed to *Mtb*; Placebo, animals exposed to *Mtb*; $C_4.T_4$, *Mtb*-exposed animals treated with $C_4.T_4$. Data are mean ± SEM and are from 3 independent experiments (n = 4 mice/group). Data were analyzed by one-way ANOVA repeated measure $^{**}p \le 0.01$, $^{***}p \le 0.001$, $^{****}p \le 0.0001$.

confocal microscopy (Figure 7C). As expected, $C_4.T_4$ induced autophagy was inhibited by PtdIns3K and autophagy inhibitors (Ly294002 and 3MA, respectively) (Figure 7D). Rapamycin was used as a positive control (Figure 7D). We also determined that CLEC4E and TLR4 pathways were MTOR-independent (Figure 7E). Taken together, these results provided evidence that the induction of autophagy in macrophages through $C_4.T_4$ signaling was linked with the MTOR-independent PtdIns3K pathway.

Previous reports suggested that a MYD88-dependent pathway is involved in both CLEC4E and TLR4 signaling [68–70]. We found that MYD88 expression was induced by both CLEC4E and TLR4 signaling (Figure 7F) and that MYD88 signaling was important for the induction of autophagy. Western blot results depicted abrogation of the conversion of LC3-I to LC3-II when $M\varphi^{C4.T4}$ were cultured with a MYD88 inhibitor (Figure 7G). These results indicated that $C_4.T_4$ activated macrophages through MYD88-mediated, MTOR-independent activation of the PtdIns3K pathway, which led to the induction of autophagy and inhibition of *Mtb* growth.

Abrogation of autophagy negated $C_4.T_4$-mediated restriction of Mtb *growth in macrophages*

BECN1 is a master regulator of autophagy [64]. To confirm that $C_4.T_4$ mediated killing of *Mtb* through autophagy, we knocked down *Becn1* expression in macrophages (Figure 7H), or inhibited autophagy with 3MA. $C_4.T_4$-induced clearance ($p < 0.0001$) of *Mtb* was abolished

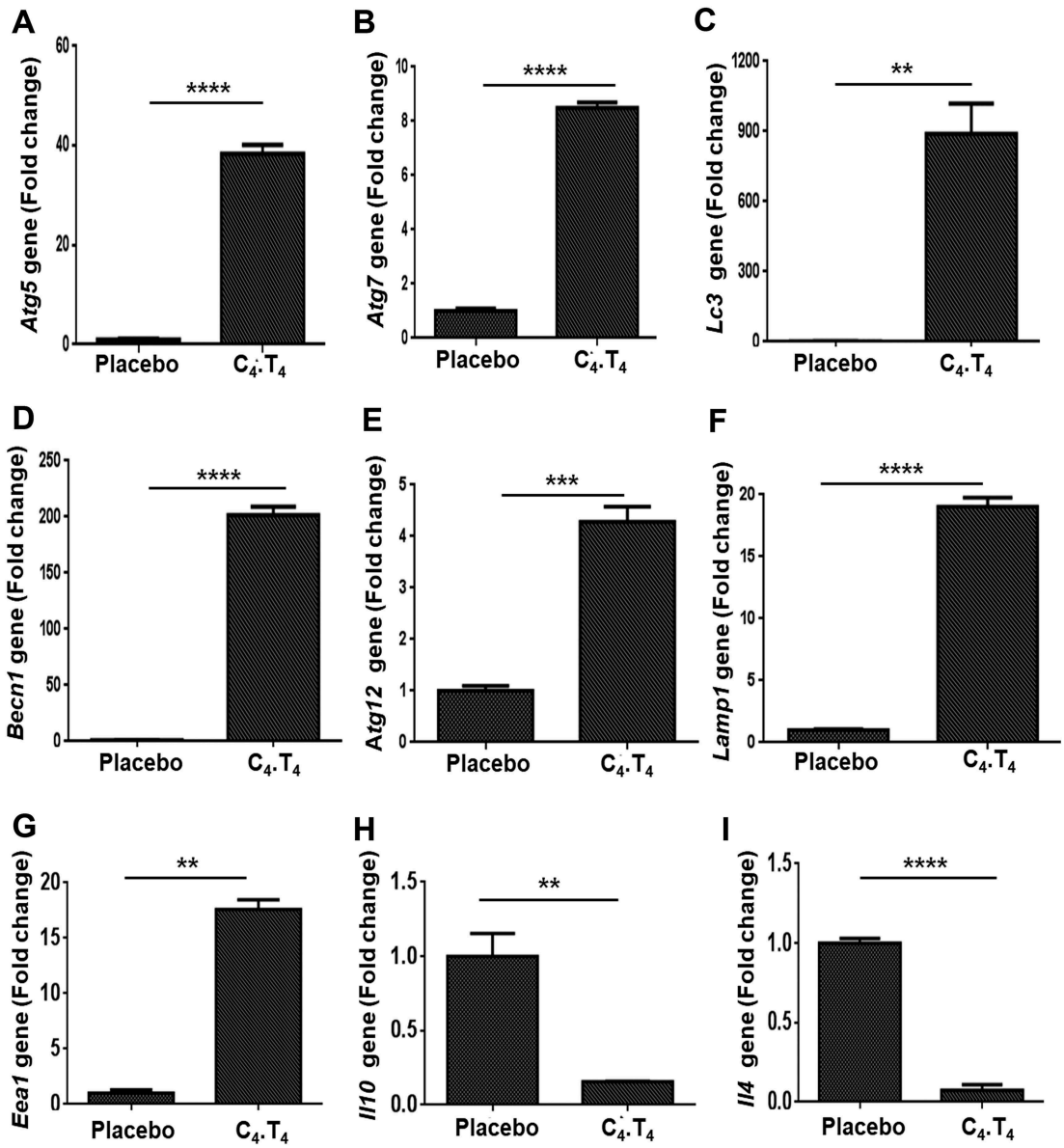

Figure 6. Signaling through $C_4.T_4$ agonists induced autophagy *in vivo*. *Mtb*-challenged animals were treated with $C_4.T_4$ and RNA was isolated from lung cells. Quantitative RT-PCR was performed to monitor the expression of (A) *Atg5*; (B) *Atg7*; (C) *Lc3*; (D) *Becn1*; (E) *Atg12*; (F) *Lamp1*; (G) *Eea1*; (H) *Il10*; (I) *Il4*. Placebo, animals exposed to *Mtb*; $C_4.T_4$, *Mtb*-exposed animals treated with $C_4.T_4$. Data are the mean ± SEM from 3 independent experiments, performed in triplicate wells. Data were analyzed by unpaired Student's "t" test ** $p \leq 0.01$, ***$p \leq 0.001$, ****$p \leq 0.0001$.

upon *Becn1* knockdown (Figure 7I). Similar results were obtained if macrophages were treated with 3MA (Figure 7I) or if macrophages from *atg5* knockout (*atg5*$^{fl/fl}$-*Lyz2/LysM-Cre*) mice were used, confirming that $C_4.T_4$-mediated elimination of *Mtb* was through autophagy (Figure 7J).

Importantly, we found significantly ($p < 0.0001$) reduced *Mtb* burden in $C_4.T_4$-stimulated human THP-1 macrophages as well (Figure S11C). $C_4.T_4$-mediated *Mtb* growth was inhibited after treatment with an autophagy inhibitor. These data confirmed that $C_4.T_4$ induced autophagy decreased *Mtb* burden in both murine and human macrophages (Figure 7I,J and S11C).

Stimulation of macrophages with $C_4.T_4$ augmented the clearance of Mtb *in macrophages through the autophagic flux*

We next studied the induction of autophagy in *Mtb*-infected macrophages by microscopy. We noted increased co-localization of GFP-*Mtb* with LC3 (GFP/green; LC3/red fluorescence) and increased LC3 puncta in the $C_4.T_4$ treated macrophages (Figure 8A). There was also an increased number of lysosomes and *Mtb* co-localization with lysosomes by immunostaining of LAMP1 (lysosomal-associated membrane protein 1) (Figure 8B). Furthermore, to confirm the presence of *Mtb* in lysosomes, we performed LysoTracker Red staining and

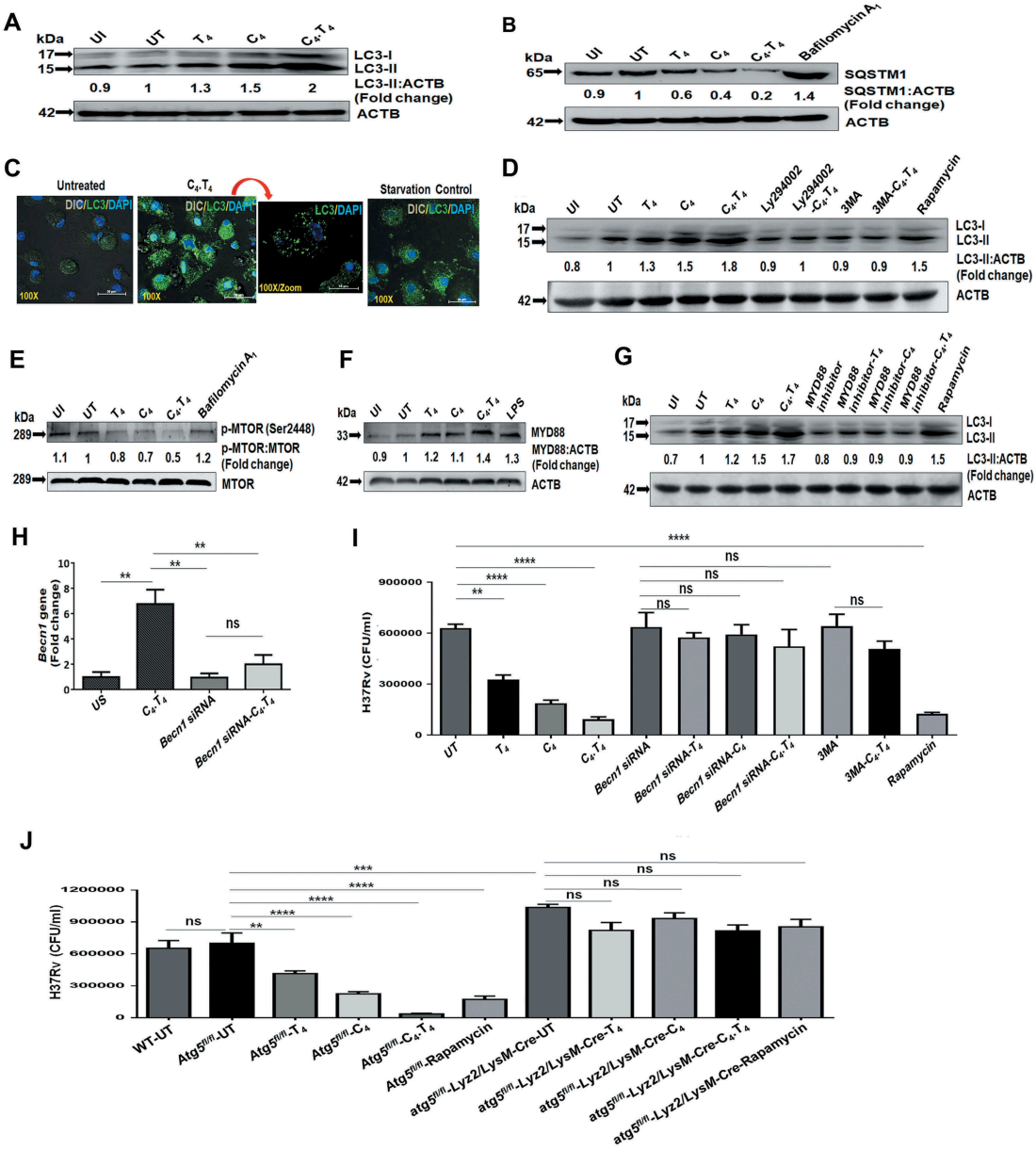

Figure 7. Signaling of *Mtb*-infected macrophages through $C_4.T_4$ induced autophagy flux through the PtdIns3K pathway. BMDMs were infected with H37Rv for 4 h, then stimulated with CLEC4E (C_4 [24 µg/ml]) and TLR4 (T_4 [10 ng/ml]) individually or in combination ($C_4.T_4$) for 4 h and checked for the (A) conversion of LC3-I to LC3-II and (B) expression of SQSTM1/P62 by western blot. Bafilomycin A_1 was used as a lysosomal enzymatic activity inhibitor, which prevents the degradation of autophagosomes. (C) Uninfected BMDMs stimulated with $C_4.T_4$ for 4 h were stained for the expression of LC3 puncta formation with anti-LC3 Abs (green). The nucleus was stained with DAPI (blue). Scale bar: 20 µm. (D) The specificity of the induction of autophagy was determined by blocking PtdIns3K to inhibit autophagy (Ly294002 and 3MA). Rapamycin was used as a positive control for autophagy and ACTB was a loading control. (E) Phosphorylation of MTOR was measured by western blot. Fold change was calculated relative to UT controls. (F,G) Infected BMDMs were treated with a MYD88 inhibitor (pepinh-MYD) for 1 h and then stimulated with $C_4.T_4$ for 4 h. (F) Expression of MYD88 and (G) conversion of LC3-I to LC3-II was observed by western blot. Data are representative of 3 independent experiments. (H,I) BMDMs were treated with *Becn1* specific siRNA for 72 h, and then cells were infected with *Mtb* for 4 h. *Becn1* expression was determined by (H) RT-qPCR. (I) *Becn1* specific siRNA treated BMDMs were infected with H37Rv for 4 h and treated with the autophagy inhibitor 3MA for 1 h. Then the cells were stimulated with $C_4.T_4$ for 48 h. Infected macrophages were lysed and CFUs were enumerated after 21 d. CFU assay showed the blocking of autophagy by siRNA or its inhibitor 3MA, increased the survival of *Mtb*. Data are presented as the mean ± SEM and are from 3 independent experiments. (J) BMDMs were collected from wild type (WT), *atg5* knockout (*atg5*$^{fl/fl}$-*Lyz2/LysM-Cre*), control flox (*Atg5*$^{fl/fl}$) mice and infected with H37Rv. The cells were then stimulated with $C_4.T_4$ for 48 h. Infected macrophages were lysed and CFUs were enumerated after 21 d. Data are presented as the mean ± SEM and are from 2 independent experiments. ns, non-significant; UI, uninfected; UT, untreated and *Mtb*-infected; C_4, CLEC4E agonist (TDB); T_4, TLR4 agonist (ultra-pure LPS). Data were analyzed by one-way ANOVA repeated measure ** $p \leq 0.01$, *** $p \leq 0.001$, **** $p \leq 0.0001$.

observed co-localization of GFP-*Mtb* with acidic vacuoles in $M\varphi^{C4.T4}$ (Figure 8C). These data provided further evidence that the improved clearance of *Mtb* in $C_4.T_4$-treated macrophages was through a xenophagy process (the autophagy-mediated clearance of pathogens).

One hallmark of autophagy is an increase in acidic vesicular organelles (AVOs) in the cytosol [71]. Our data show an increased number of AVOs in *Mtb*-infected $M\varphi^{C4.T4}$ that is specific to autophagy since there is a decrease in the frequency of AVOs with 3MA inhibitor treatment (Figure 9A,B). The

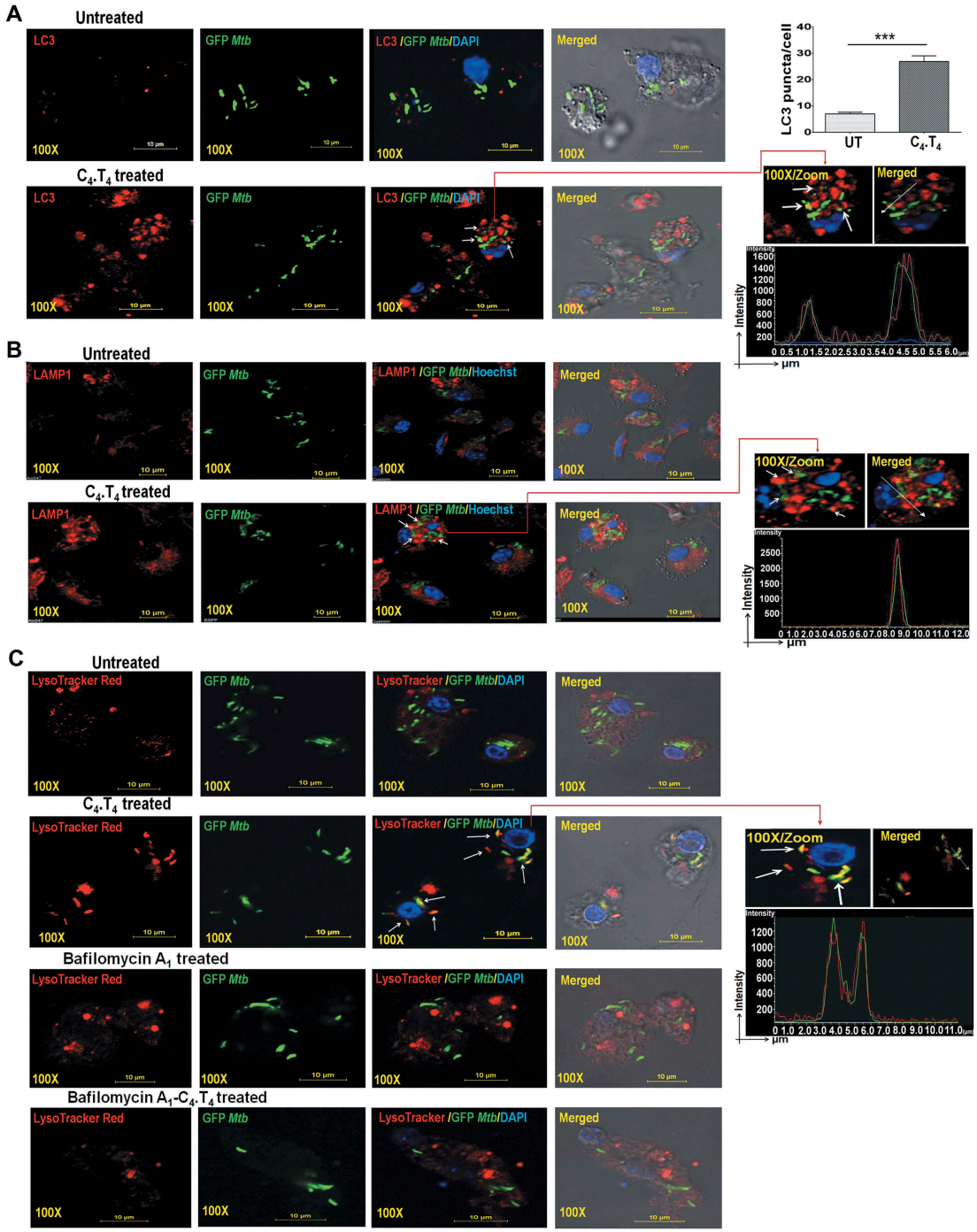

Figure 8. Stimulation of *Mtb*-infected macrophages by $C_4.T_4$ induced autophagy flux and enhanced the number of autolysosomes and transported *Mtb* to the lysosomes of macrophages. BMDMs were infected with GFP-*Mtb* for 4 h then stimulated with $C_4.T_4$ for 4 h and 10 h. The cells were immunostained with anti-LC3 and anti-LAMP1 Abs along with DAPI or Hoechst to visualize nucleus (blue) and examined for the formation of (A) autophagosomes (red) and (B) lysosomes/autolysosomes (red). (C) BMDMs were infected with GFP-*Mtb*for 4 h and stimulated with $C_4.T_4$ for 10 h. LysoTracker Red staining was performed to monitor acidic vacuoles and LysoTracker co-localization with GFP-*Mtb* by confocal microscopy. The histogram data (green and red) showed the co-localization of GFP-*Mtb* (green) with LC3 (red) or LAMP1 (red) or LysoTracker (red) in $C_4.T_4$-treated macrophages indicated by white arrows. Scale bar: 10 μm and 100X magnification. (A) The bar diagram showed the number of LC3 puncta/cell. The LC3-II puncta in each cell were counted in 10 different fields. Quantification of the LC3 puncta per cell are presented as the mean ± SD. UT, untreated and GFP-*Mtb*-infected; $C_4.T_4$, $C_4.T_4$ treated and GFP-*Mtb*-infected. The data are representative of 4 independent experiments. Data were analyzed by unpaired Student's "t" test *** $p \leq 0.001$.

data were substantiated using monodansylcadaverine (MDC) staining, which is a specific dye for locating acidic compartments (Figure 9C). Therefore, these data suggested that CLEC4E and TLR4 signaling in macrophages enhanced acidic vacuole formation. We also performed intracellular staining of LAMP1 in the macrophages treated with $C_4.T_4$ by flow cytometry. A significantly ($p < 0.01$) higher accumulation of LAMP1 in $M\varphi^{C4.T4}$ was seen (Figures 9D,E and S12), which was further validated by staining $M\varphi^{C4.T4}$ with LysoTracker Red dye (Figure 9F).

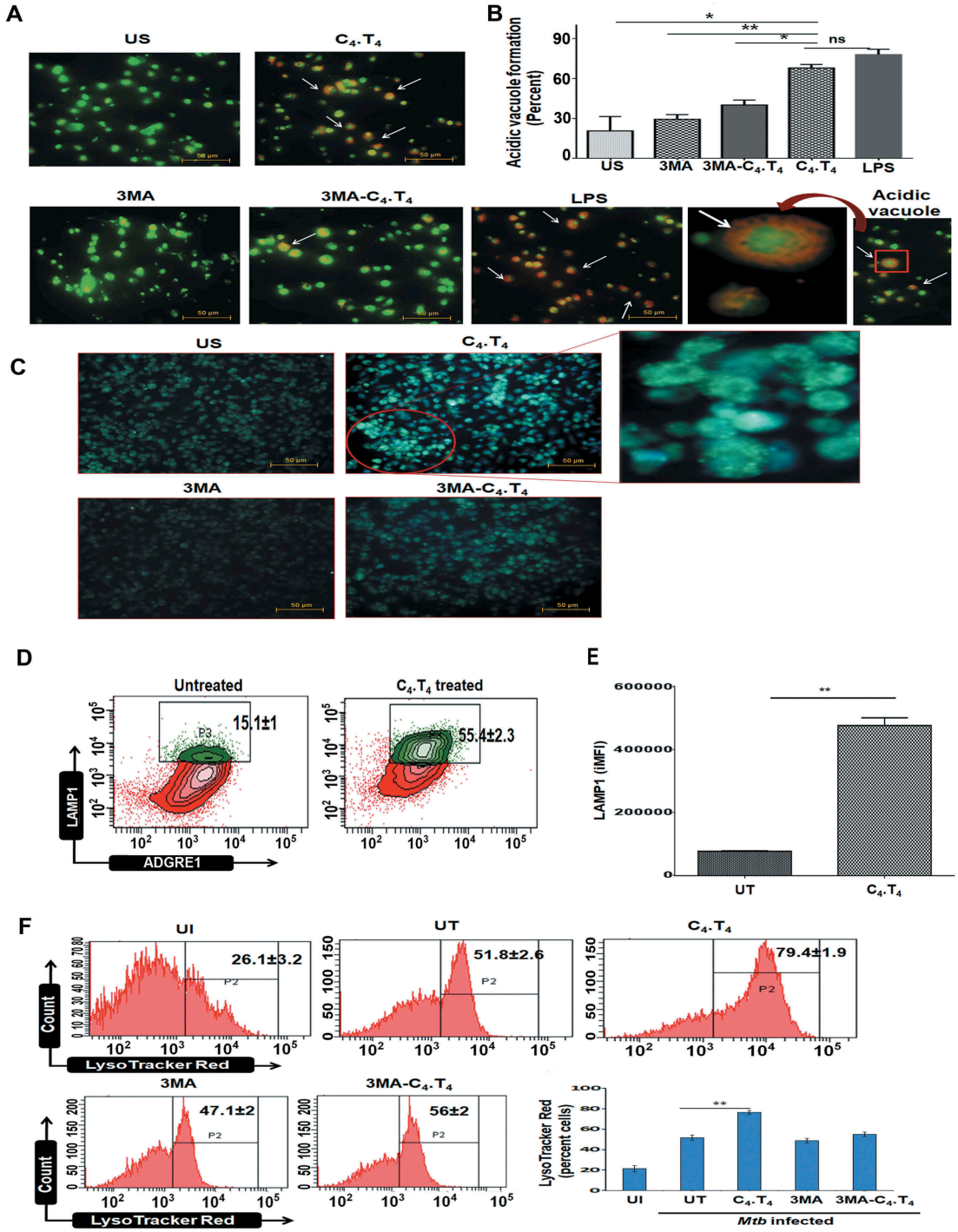

Figure 9. Activation of macrophages through $C_4.T_4$ induced autophagosome and lysosome formation. BMDMs were treated with 3MA (10 mM) for 1 h. Next, they were stimulated with $C_4.T_4$ for 4 h and the cells were stained with (A,B) acridine orange or (C) MDC to monitor the acidic compartments by fluorescence microscopy. Scale bar: 50 µm and 20X magnification. (B) The number of acidic vacuoles in each cell was counted in 4 individual fields for each group. White arrows indicated lysosomal acidification (orange). LPS was used as a positive control for acidic vacuoles formation and 3MA was a negative control for autophagosomes formation. Data were analyzed by one-way ANOVA repeated measure *p ≤ 0.05, ** p ≤ 0.01. Late endosomal-lysosomal acidification was assessed through (D,E) LAMP1 staining by flow cytometry; data were expressed as a bar diagram (E). Numbers in the inset of contour plots depicted the percentage of cells. The integrated MFI (iMFI) is calculated by multiplying the relative frequency (% positive population) of cells expressing LAMP1 with the mean fluorescence intensity (MFI) of that population. (F) BMDMs were infected with GFP-*Mtb*for 4 h. Next, the cells were treated with 3MA (10 mM) for 1 h and then stimulated with $C_4.T_4$ for 10–12 h. Control cultures were kept without 3MA. The cells were stained with LysoTracker Red dye and monitored by flow cytometry. US, unstimulated; UI, uninfected cells; UT, untreated and *Mtb*-infected cells. Scale bar: 10 µm. 100X magnification. Data are expressed as mean ± SEM and are from 3 independent experiments. Data were analyzed by unpaired Student's "t" test ** p ≤ 0.01.

CLEC4E and TLR4 signaling induced phosphorylation of PtdIns3K and STAT1 and nuclear translocation of RELA/NFKB

Activating macrophages with $C_4.T_4$ augmented NOS2 (nitric oxide synthase 2, inducible), IL6, TNF, and IL1B production. These molecules play important roles in the activation of different transcription factors like RELA/NFKB. We observed increased STAT1 and PtdIns3K phosphorylation in *Mtb*-infected $M\varphi^{C4.T4}$ (Figure 10A,B). The PtdIns3K inhibitor LY294002 was used as a control (Figure 10B). Interestingly, we observed decreased STAT6 phosphorylation in $M\varphi^{C4.T4}$ (Figure S13A). CLEC4E and TLR4 may enhance the survival of macrophages. We noticed increased levels of the anti-apoptotic molecule BCL2L1/Bcl-xL in $M\varphi^{C4.T4}$ (Figure 10C).

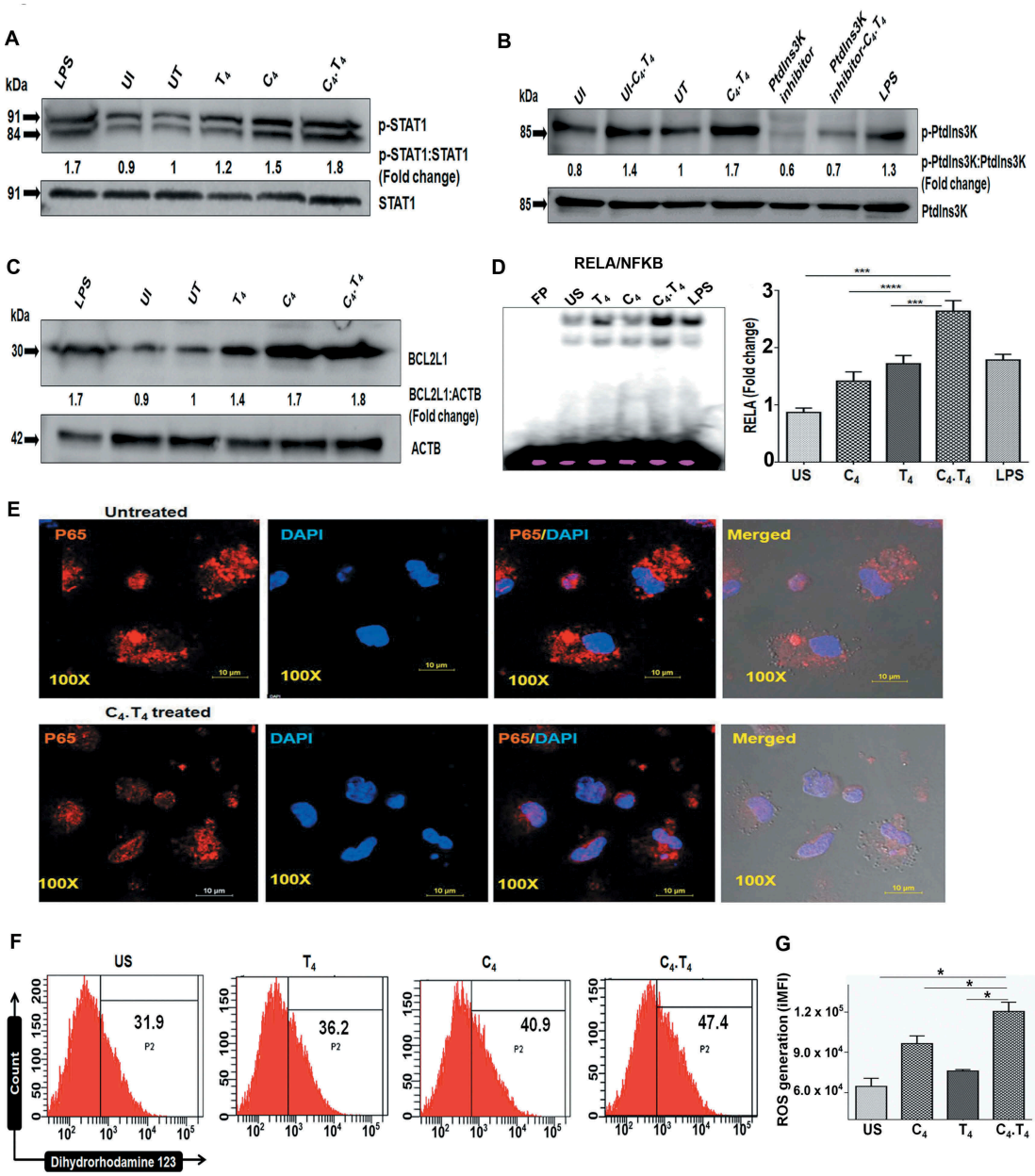

Figure 10. $C_4.T_4$ induced phosphorylation of STAT1, PtdIns3K and enhanced nuclear translocation of RELA/NFKB. Macrophages were infected with H37Rv for 4 h and cultured with $C_4.T_4$ for 15–30 min and 24 h. The cell lysate was prepared, and western blot was performed to monitor the expression of (A) p-STAT1; (B) p-PtdIns3K; (C) BCL2L1. The densitometry data represent fold change. The ratio for untreated cells was considered to be 1. LPS was used as a positive control. UI, uninfected; UT, untreated and *Mtb*-infected; C_4, CLEC4E agonist (TDB); T_4, TLR4 agonist (ultra-pure LPS). The data are representative of 2–3 independent experiments. (D–G) BMDMs were stimulated with C_4 (24 μg/ml) and T_4 (10 ng/ml) individually or in combination ($C_4.T_4$) for 30 min. (D) Nuclear translocation of RELA/NFKB was monitored by EMSA. The data were graphed as fold change in the form of a bar diagram. Unstimulated cells were considered as 1. FP, free probe; US, unstimulated. The data are shown as the mean ± SEM and are from 2 independent experiments. Data were analyzed by one-way ANOVA repeated measure. ***$p \le 0.001$, ****$p \le 0.0001$. (E) Translocation of RELA/NFKB p65 into the nucleus was further monitored by confocal microscopy and (F,G) the generation of ROS was observed by flow cytometry after labeling with dihydrorhodamine 123 dye. (F) The histogram depicted ROS generation (percentage). (G) The bar diagram represented integrated MFI of ROS generation. The data represented in each histogram or contour plot depicted the percentage of cells from the ADGRE1/F4/80 gated population. US, unstimulated; UT, untreated and *Mtb*-infected; C_4, CLEC4E agonist (TDB); T_4, TLR4 agonist (ultra-pure LPS). The integrated MFI (iMFI) is calculated by multiplying the relative frequency (% positive population) of cells generating ROS with the mean fluorescence intensity (MFI) of that population. Data are shown as the mean ± SD and are representative of 2–3 independent experiments. Data were analyzed by one-way ANOVA repeated measure. *$p \le 0.05$.

Furthermore, there was downregulation in the expression of negative regulators of immunity like FAS, HAVCR2/TIM-3, and CD274/PD-L1 (Figure S13B–D). This phenotype denoted a possibility of better survival of $M\varphi^{C4.T4}$.

Signaling through CLEC4E *via* SYK induces reactive oxygen species (ROS) generation [72], which can directly activate RELA/NFKB [72–74]. RELA/NFKB is responsible for cellular growth and inflammatory responses. Considering all these facts, we monitored RELA/NFKB activation in $M\varphi^{C4.T4}$. Interestingly, we observed increased ($p < 0.0001$) RELA/NFKB activation and translocation into the nucleus, by EMSA (Figure 10D). We confirmed these results by confocal microscopy (Figure 10E). In addition, we noted increased ($p < 0.05$) ROS generation by flow cytometry (Figure 10F,G). Therefore, it can be concluded that $C_4.T_4$ signaling involved ROS and RELA/NFKB pathway, which may be responsible for the activation of macrophages. We also monitored NOS2 expression and NO release by $M\varphi^{C4.T4}$, since NO mediates killing of intracellular *Mtb* in murine macrophages [75,76]. Our western blot results indicated that $C_4.T_4$ enhanced the expression of NOS2, as compared to controls (Figure S14A). We confirmed that this change correlated with increased NO release and validated the specificity of the results by blocking the production of NO by its inhibitor N-mono-methyl L-arginine (NM). Decreased ($p < 0.001$) $C_4.T_4$-stimulated NO release was observed with NM treatment (Figure S14B). Notably, we observed significantly ($p < 0.05$) enhanced NO secretion from the cells isolated from the lungs of $C_4.T_4$ injected *Mtb*-challenged mice (Figure S14C). RT-qPCR performed on the same lung tissues revealed a significant ($p < 0.01$) augmentation in *Nos2* gene expression in the mice administered $C_4.T_4$ (Figure S14D). Therefore, the results indicated that $C_4.T_4$-mediated killing of *Mtb* could occur through autophagy, as well as ROS and NO production.

Overall, the study provided evidence that combinatorial signaling through CLEC4E and TLR4 activated macrophages *via* the MYD88-PtdIns3K-STAT1-RELA/NFKB pathway that ultimately leads to the induction of autophagy to control the growth of *Mtb* (Figure 11A,B).

Discussion

Modulation of host immunity can be an efficacious approach to successfully eliminate pathogens. Several innate immune receptors such as TLRs, CLRs, NLRs and RLRs can effectively bolster immunity against an array of pathogens [48,49,77–80]. Among the molecules that stimulate innate immunity, a TLR4 agonist has been considered a potential immunotherapeutic due to its ability to stimulate the immune system against several pathogens [32,33]. Additionally, CLEC4E is a promising vaccine adjuvant in modulating immunity against chronic *Mtb* infection [77,78]. There are no studies demonstrating the mechanistic role of CLEC4E and TLR4 agonist-mediated combinatorial signaling in imparting immunity against *Mtb*. The role of CLEC4E in inducing autophagy is totally unexplored. Therefore, we studied both *in vitro* and *in vivo* efficacy of CLEC4E and TLR4 on the activation of *Mtb*-infected macrophages. The macrophages exhibited the following major changes: i) enhanced release of cytokines, up-regulated expression of the costimulatory molecules such as CD40, CD86 and H2/MHC-II, and down-regulated inhibitory molecules such as FAS, HAVCR2/TIM-3, and CD274/PD-L1; ii) the phenotype of $M\varphi^{C4.T4}$ ($IL6^{hi}$, $IL12B^{hi}$, TNF^{hi}, $IL1B^{hi}$, $IFNG^{hi}$, $IL17A^{hi}$, NO^{hi}, $IL10^{lo}$) suggested their enhanced capability to kill *Mtb*; iii) reduced dose and increased potency of anti-TB drugs to kill *Mtb*; iv) improved ability to activate *Mtb*-specific T cells and generate Th1 cells and Th17 cells; v) expanded pool of memory T cells; vi) induced MYD88, PtdIns3K, STAT1, and RELA/NFKB pathways; vii) restricted survival of *Mtb* through autophagy. These data provide sufficient evidence for a novel role of CLEC4E and TLR4 in boosting the function of macrophages to kill *Mtb*.

The currently available regime to treat TB patients is highly effective but the major drawbacks are its adverse side-effects, immune-suppression, long-duration of treatment and emergence of drug resistance in *Mtb* [81–84]. Our study showed that adjunct therapy of anti-TB drugs (RIF and INH) with $C_4.T_4$ agonists dramatically improved their potency to kill *Mtb*. Notably, we achieved better killing of the bacterium with 10-fold lower dose of rifampicin along with $C_4.T_4$, as compared to the drug alone. This observation suggested an immunomodulatory role of $C_4.T_4$ in reducing the dose as well as duration of anti-TB drugs. $C_4.T_4$ will bolster host immunity against the pathogen and thereby provide an added advantage for the drug to act more efficiently in killing the bacterium, and consequently, may minimize the opportunity for the bacterium to develop drug resistance.

Both CD4- and CD8A-positive T cells protect against *Mtb* [85]. We observed that $C_4.T_4$ therapy enhanced CD4-positive T cells and CD8A-positive T cells proliferation. Furthermore, Th1 cells and Th17 cells played an important role in protection against *Mtb*. In contrast, Th2 cells support the propagation of *Mtb* [86]. Excitingly, an expanded pool of Th1 cells and Th17 cells but not Th2 cells was noted in the animals that were treated with $C_4.T_4$. The same group of animals showed significant clearance of *Mtb* from the lungs and reduced its dissemination to the spleen and liver. The presence of polyfunctional Th1 and Th17 cells, which provide better protection against pathogens when compared to their counterparts secreting a single cytokine [53–55], further supports the role of $C_4.T_4$ therapy against *Mtb*. Memory T cells induce long-lasting protection [87,88]. $C_4.T_4$ significantly enhanced the pool of memory T cells in the same animals that exhibited decreased *Mtb* burden, signifying the generation of immunological memory to protect from subsequent *Mtb* infection.

There are growing evidences that autophagy helps to protect against many diseases [47,60,61,89]. The contribution of autophagy during *Mtb* infection has been well-defined as autophagy induction or inhibition controls and enhances *Mtb* growth, respectively, and *Mtb* co-localizes with autophagy factors ATG5, ATG12, SQSTM1, BECN1 and LC3 [90–93]. In contrast, a previous report shows autophagy-independent functions of ATG5 in different experimental settings *in vivo* [94–96]. Autophagy can control *Mtb* through multiple mechanisms: it targets the antigen for lysosomal degradation and improves antigen processing and presentation to T cells [97]. Concurrently, it inhibits the excessive inflammatory response [37,60]. Notably, $C_4.T_4$-treated mice showed

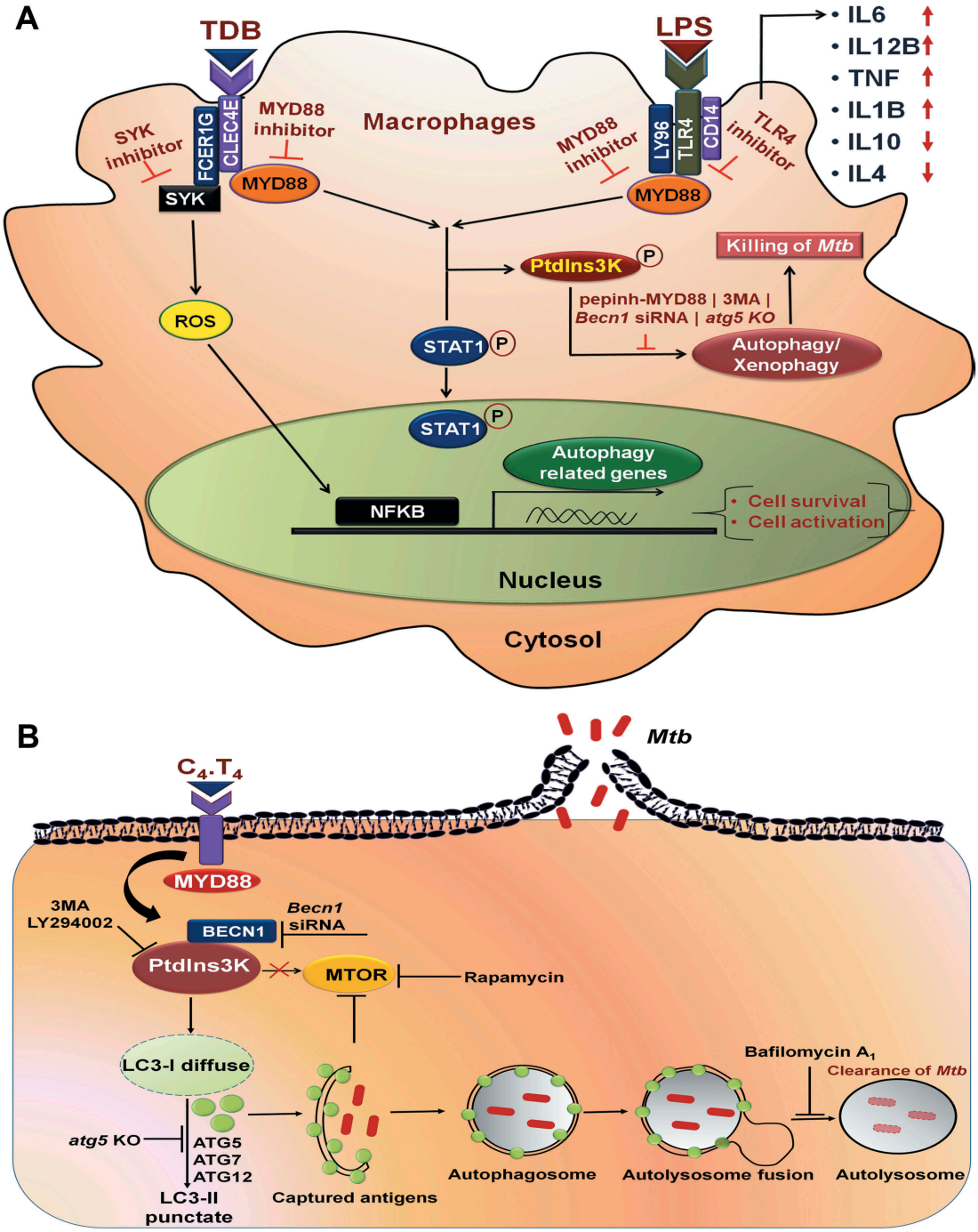

Figure 11. Proposed mechanism of signaling pathways initiated by $C_4.T_4$ in macrophages. (A) $C_4.T_4$ signaling activated RELA/NFKB through MYD88 pathway and enhanced cytokine secretion, which received positive feedback through phosphorylated PtdIns3K, STAT1 and activated BCL2L1. Consequently, these macrophages induced autophagy, activated cells, and increased cell survival. This mechanism played a key role in controlling the growth of *Mtb*. (B) Schematic representation of $C_4.T_4$-mediated clearance of *Mtb* through modulation of autophagy and lysosomal biogenesis.

enhanced autophagy and autophagic flux. Additionally, expression of autophagy-related genes was increased, which correlated with a decreased number of *Mtb*. Blocking of autophagy (through reduced BECN1 or ATG5 expression) rescued *Mtb* growth. These results provided strong support for the involvement of autophagy in combating *Mtb* in mice that were administered $C_4.T_4$.

Following ligand binding, CLEC4E interacts with FCER1G/FcRγ chain, then phosphorylates and activates SYK [72]. This activation induces ROS generation and CARD9-mediated RELA/NFKB activation; which leads to IL6, TNF and IL1B secretion [72–74]. TLR4 signaling activates the conventional MYD88-mediated pathway, leading to RELA/NFKB activation and cytokine production, which may contribute to a positive feedback loop. Consequently, PtdIns3K becomes activated, which induces a survival signal and autophagy. We observed involvement of the MYD88 pathway and induction of autophagy in CLEC4E signaling. Activation of PtdIns3K delivered a signal through RELA/NFKB and BCL2L1. Interestingly, we noticed that signaling through C_4.

T_4 activates RELA/NFKB and augments production of IL6, IL12B, TNF, and IL1B, consequently delivering a feedback mechanism through STAT1 phosphorylation that supported the activation and survival of $M\varphi^{C4.T4}$.

Overall, we have elucidated a novel signaling network operating through $C_4.T_4$ (Figure 11). Signaling *via* $C_4.T_4$ activated RELA/NFKB through MYD88-mediated phosphorylation of PtdIns3K, STAT1 and release of NO. Signaling through $C_4.T_4$ activated macrophages and induced autophagy to effectively control *Mtb* infection. In the future, treatment with $C_4.T_4$ agonists alone or as an adjunct therapy with anti-TB drugs may be an important new host-directed strategy to treat TB patients.

Materials and methods

Animals

C57BL/6 mice, 6–8 weeks were obtained from the institute's animal facility. Guinea pigs (6–8 weeks) were purchased from the CCS Haryana Agricultural University, Hisar, India. *Atg5*$^{fl/fl}$ and *atg5*$^{fl/fl}$*-Lyz2/LysM-Cre* mice bones were kindly provided by Dr. Christina L. Stallings, Department of Molecular Microbiology, Washington University School of Medicine, St Louis, MO.

Ethics statement

All the experiments were approved by the Institutional Animal Ethics Committees (IAEC) of the Institute of Microbial Technology (IMTECH), Chandigarh and International Center for Genetic Engineering and Biotechnology (ICGEB), New Delhi. The experiments were accomplished according to the National Regulatory Guideline issued by Committee for the Purpose of Control and Supervision of Experiments on Animals (No. 55/1999/CPCSEA), Ministry of Environment and Forest, Government of India. Mice experiments were performed at IMTECH and guinea pigs at the ICGEB. The *atg5* knockout experiments were performed at Texas Biomedical Research Institute, San Antonio, TX, USA. The experiments were approved by the Texas Biomedical Research Institute, Institutional Animal Care and Use Committee (IACUC).

Antibodies and reagents

Agonist of CLEC4E (TDB, tlrl-tdb), TLR4 (LPS EK ultrapure, tlrl-peklps), SYK inhibitor (Piceatannol, tlrl-pct), TLR4 signaling inhibitor (CLI-095, tlrl-cli95) and MYD88 inhibitor (Pepinh-MYD, tlrl-pimyd) were purchased from InvivoGen.

Antibodies (Abs) and reagents used in western blotting: phospho-PI3 kinase p85 (Cell Signaling Technology, 4228S), PI3 kinase p85 (Cell Signaling Technology, 4257S), BCL2L1/Bcl-xL (Cell Signaling Technology, 2762S), pMTOR (Ser2448; Cell Signaling Technology, 5536S), MTOR (Cell Signaling Technology, 2983S), p-STAT6 (Cell Signaling Technology, 56554S), STAT6 (Cell Signaling Technology, 5397S), RELA/NFKB-p65 (Cell Signaling Technology, 8242S) and MYD88 (Cell Signaling Technology, 4283S), SQSTM1/p62 (Santa Cruz Biotechnology, sc-48402), NOS2/iNOS (Abcam, ab3523). Other reagents were procured from the specified companies: inhibitors against PtdIns3K (Ly294002; Sigma Aldrich, 440202) and NOS2 [NM] (Calbiochem, 475886), FlexiTube siRNA-specific for mouse *Becn1* (Qiagen, GS56208), acridine orange (Sigma Aldrich, A6014), monodansylcadaverine (Sigma Aldrich, D4008), rabbit polyclonal Ab against LC3 (Sigma Aldrich, L8918), anti-ACTB antibody (Sigma Aldrich, A1978), p-STAT1 (BD Pharmingen, 612232), STAT1 (BD Pharmingen, 610115), LysoTracker Red (Life Technologies, L-7528), antifade reagent (Life Technologies, P36934), dihydrorhodamine 123 (Sigma Aldrich, D1054), 4′,6-diamidino-2-phenylindole dihydrochloride (DAPI; Sigma Aldrich, D8417), 3-methyladenine (3MA; Sigma Aldrich, M9281), rapamycin (Sigma Aldrich, B1793), 5(6)-carboxyfluorescein diacetate N-succinimidyl ester (CFSE; Sigma Aldrich, 21888F), phorbol 12-myristate 13-acetate (PMA; Calbiochem, 524400), DMSO (Sigma Aldrich, D8418), RELA/NFKB consensus oligonucleotide (Promega, E3292), paraformaldehyde (Sigma Aldrich, P6148), Griess reagent (Sigma Aldrich, G4410), poly-L-lysine solution (Sigma Aldrich, P8920), HBSS (GIBCO, 14185052), isoniazid (Sigma Aldrich, 13377), rifampicin (Sigma Aldrich, R3501), bovine serum albumin (BSA) (Sigma Aldrich, A0281), Triton™ X-100 solution (Sigma Aldrich, 93443), glycerol (Sigma Aldrich, G5516), TWEEN 20 (Sigma Aldrich, P9416), TWEEN 80 (Sigma Aldrich, P4780), avidin–peroxidase (Sigma Aldrich, A7419), o-Phenylenediamine (Sigma Aldrich, P9029), Middlebrook 7H9 broth (Difco-Becton Dickinson, 271310), Middlebrook 7H11 agar (Difco-Becton Dickinson, 283810), Middlebrook OADC growth supplement (Sigma Aldrich, M0678), saponin (Sigma Aldrich, 84510), PVDF western blotting membranes (Sigma Aldrich, 3010040001), amikacin hydrate (Sigma Aldrich, A3650), sodium nitrite (Sigma Aldrich, 237213), phenylmethanesulfonyl fluoride (PMSF; Sigma Aldrich, 78830), protease and phosphatase inhibitor cocktail (Sigma Aldrich, PPC1010).

All other reagents and chemicals were procured from the following companies. Free or fluorochrome-conjugated Abs: Purified anti-mouse FCGR3/FCGR2B Ab (eBioscience, 14-0161-86), CD80-FITC (BD Pharmingen, 553768), ADGRE1/F4/80-APC (eBioscience, 14-4801-82), F4/80-PerCP-Cyanine5.5 (eBioscience, 45-4801-82), CD40-PE-Cyanine5 (eBioscience, 15-0401-82), CD86-PE (eBioscience, 12-0862-85), H2/MHC-II-PerCPefluor710 (eBioscience, 46-5321-82), FAS/CD95-FITC (BD Pharmingen, 561979), CD274/PD-L1-PE (eBioscience, 12-5982-83), HAVCR2/CD366/TIM3-APC (eBioscience, 17-5871-82), LAMP1/CD107a-Alexa Fluor 647 (BioLegend, 121610), ANXA5 (annexin A5)-FITC (BioLegend, 640906), propidium iodide (Sigma Aldrich, P4170), CD4-Pacific Blue (BD Pharmingen, 558107), CD8A-APC-Cy7 (BD Pharmingen, 557654), IFNG-PE-Cyanine7 (eBioscience, 25-7311-82), IL17A-PE (BioLegend, 506904), SELL/CD62L-FITC (BD Pharmingen, 553150), IL7R/CD127-PE-Cyanine5 (eBioscience, 15-1271-83), CD44-PerCP/Cyanine5.5 (eBioscience, 45-0441-82), CCR7-PE-Cyanine7 (eBioscience, 25-1971-82), TNF-PerCP-Cyanine5.5 (BioLegend, 506322), Alexa fluor 633-anti-rabbit secondary Ab (Invitrogen, A-21071), Alexa fluor 488-anti-rabbit secondary Ab (Invitrogen, A-11034). Other reagents: Dulbecco's phosphate-buffered saline (DPBS/PBS) (GIBCO, 14190-144), Roswell Park Memorial

Institute (RPMI)-1640 (GIBCO, 11875-093) and Fetal bovine serum (FBS; GIBCO, 10082-147), L-pyruvate (SERVA, 15220), L-glutamine (SERVA, 22942), streptomycin (SERVA, 35500), penicillin (SERVA, 31749). ELISA Abs: purified anti-mouse IL6 (BD Pharmingen, 554400), biotin anti-mouse IL6 (BD Pharmingen, 554402), recombinant mouse IL6 (BD Pharmingen, 554582), purified anti-mouse IL12B (BD Pharmingen, 551219), biotin anti-mouse IL12B (BD Pharmingen, 554476), recombinant mouse IL12B (BD Pharmingen, 554592), purified anti-mouse TNF (BD Pharmingen, 551225), biotin anti-mouse TNF (BD Pharmingen, 554415), recombinant mouse TNF (BD Pharmingen, 554589), purified anti-mouse/rat IL1B (BioLegend, 503502), biotin anti-mouse TNF (BioLegend, 515801), recombinant mouse IL1B (BioLegend, 575109), purified rat anti-mouse IL10 (BD Pharmingen, 551215), biotin rat anti-mouse IL10 (BD Pharmingen, 554465), recombinant mouse IL10 (BD Pharmingen, 550070). The primer sequences for RT-qPCR were purchased from Sigma Aldrich. All tissue culture grade plasticware was procured from BD Biosciences, Thermo Fisher Scientific, Corning™ Costar™ or Sigma Aldrich.

Culture of bone marrow derived macrophages (BMDMs)

Briefly, bone marrow cells (BMCs) from the femurs and tibia of C57BL/6 wild type, *Atg5*$^{fl/fl}$ and *atg5*$^{fl/fl}$*-Lys2/LysM-Cre* mice were flushed aseptically. BMCs were cultured in RPMI-1640 (GIBCO, Invitrogen Life Technologies, 11875-093) containing FBS (10%) with L-glutamine (100 mM), penicillin (100 U/ml), streptomycin (100 mg/ml) and replenished with L929 cells culture supernatant (20%), as a source of macrophage colony-stimulating factor (M-CSF). The cultures were kept in a humidified atmosphere at 37°C (5% CO_2). The medium was replenished after 3 d. After 7 d, macrophages (BMDMs) (2.5×10^5/well) were harvested and cultured in 48 well tissue culture grade plates with the agonists C_4/TDB (24 μg/ml), T_4/ultra-pure LPS (10 ng/ml) or $C_4.T_4$ for 48 h with or without *Mtb* infection. For western blot and RT-qPCR experiments, BMDMs (2.5×10^6/well) were cultured in 6 well tissue culture grade plates. The cells were then infected and stimulated with C_4 (24 μg/ml), T_4 (10 ng/ml) or $C_4.T_4$ for 4–8 h.

THP-1 macrophage differentiation

THP-1 monocytes (3×10^5/well) were treated with PMA (20 ng/ml) for 16 h in 48 well plates in RPMI containing FBS (10%) at 37°C (5% CO_2). The adherent macrophages were washed with RPMI twice and then rested for another 24 h prior to stimulation with C_4 (24 μg/ml), T_4 (10 ng/ml) or $C_4.T_4$ for 48 h.

Phenotype of BMDMs

The phenotype of *Mtb*-infected BMDMs was assessed by flow cytometry. Infected macrophages were triggered with CLEC4E and TLR4 agonist ($C_4.T_4$) for 48 h. BMDMs harvested at 48 h were re-suspended in FACS buffer (2% FCS in PBS). The cells were treated with anti-FCGR3/FCGR2B Ab for 30 min at 4°C to block non-specific binding of Abs to FCGRs. Cells were then stained with fluorochrome-labeled Abs specific for mouse CD40, CD86, H2/MHC-II, FAS, CD274/PD-L1, and HAVCR3/TIM-3 or isotype-matched control Abs. Further, the cells were then fixed with paraformaldehyde (1%). Cells were washed between each step. The samples were analyzed using a FACS Aria and data analyzed with BD DIVA (BD Biosciences, San Jose, CA) and FlowJo software (Williamson Way, Ashland, OR).

Propidium iodide (PI) and ANXA5 assays

Mtb-infected BMDMs were cultured with the agonists of CLEC4E (C_4/TDB) or TLR4 (T_4/ultra-pure LPS) or CLEC4E-TLR4 ($C_4.T_4$) at 37°C (5% CO_2) for 48 h. This was followed by re-suspending cells in binding buffer (0.01 M HEPES [pH 7.4], 0.14 M NaCl and 2.5 mM $CaCl_2$). FITC-labeled ANXA5 (5 μl/tube) and 2 μl of PI (50 μg/ml) were added to the samples and then incubated in the dark at RT. After 15 min, 1X binding buffer (400 μl) was added and cells were analyzed immediately employing a BD FACS Aria flow cytometer and data analysis was performed by DIVA software.

Scanning electron microscopy (SEM)

BMDMs were stimulated with agonists of CLEC4E (24 μg/ml) and TLR4 (10 ng/ml) for 48 h. The cells were fixed on Poly-L-Lysine pre-coated coverslips with modified Karnovsky's fixative (MKF) at 4°C. After 3 h, cells were washed 3 x with PBS at 4°C. Dehydration of samples was done with 30%, 50% and 70% ethanol at the interval of 30 min at 4°C. Samples were treated with 90%, 100%-I, and 100%-II ethanol at intervals of 30 min at RT and dehydrated with tetra-butyl alcohol (TBA) twice at intervals of 30 min at RT. TBA was removed and freeze drying was performed at −120°C for 3 h and cells observed under SEM at 15 KX magnification.

Cytokine estimation

Cytokine release was measured in culture supernatants (SNs) after 48 h of $C_4.T_4$ stimulation by standard ELISA method, according to manufacturer's instructions. Macrophages (2.5×10^5/well) were incubated in 48 well plates and stimulated with the agonists C_4 (24 μg/ml), T_4 (10 ng/ml) or $C_4.T_4$. The SNs were collected after 48 h to measure IL6, IL12B, TNF, IL1B, and IL10. Briefly, 96 well plates were coated with Abs to mouse IL6 (2 μg/ml), IL12B (2 μg/ml), IL1B (2 μg/ml) and TNF (4 μg/ml), IL10 (4 μg/ml) in phosphate buffer (0.01 M-pH 9.2 and pH 6 respectively) overnight (O.N.) at 4°C. Blocking with BSA (1%) in PBS was done for 3 h at RT. Afterward, the corresponding recombinant cytokines were used as standard, and culture SNs (50 μl volume) were added and then incubated O.N. at 4°C. Biotinylated anti-mouse IL6 (2 μg/ml), IL12B (2 μg/ml), IL10 (2 μg/ml) and TNF (1 μg/ml), IL1B (1 μg/ml) Abs in BSA (1%)-PBS-TWEEN 20 buffers were added into the ELISA plates and incubated for 2 h at RT. Subsequently,

avidin-HRP (1:10,000) was added and then incubated at 37° C for 45 min. The regular procedures of incubation and washing with PBST (1XPBS-0.05% TWEEN 20) were achieved at each step. Later, the color was developed using H_2O_2-OPD substrate-chromogen. The reaction was stopped by 7% H_2SO_4 after color development. The plates were read in an ELISA reader at 492 nm. The results are expressed as pg/ml. The secreted cytokines were determined using serial log_2 dilutions of standard curve drawn using rIL6, rIL12B, rTNF, rIL1B, and rIL10.

Culturing of mycobacteria

Mycobacterium strains (H37Rv, H37Ra) were a kind gift from Dr. V.M. Katoch (National JALMA Institute for Leprosy and other Mycobacterial Diseases, Agra, India) and GFP-H37Ra, H37Rv were kindly provided by Dr. P. Gupta (IMTECH, Chandigarh, India). Unless otherwise indicated, *Mtb* H37Rv was used for all experiments. Mycobacterium strains were cultivated in Middlebrook 7H9 broth with glycerol (0.2%) and TWEEN-80 (0.05%), complemented with dextrose, catalase and albumin. The viability of *Mtb* was confirmed by colony-forming units (CFUs) on Middlebrook 7H11 medium supplemented with albumin, oleic acid, dextrose as well as catalase. CFUs were enumerated 20 d after plating.

In vitro infection with mycobacteria

BMDMs were infected with *M. smegmatis* (MOI 1:5) or *Mtb*-H37Rv/H37Ra (MOI 1:5) and harvested after 3 h and 4 h, respectively. The extracellular bacteria were removed by treating cultures with amikacin (2 μg/ml) followed by extensive washing with PBS. *M. smegmatis* and *Mtb*-infected BMDMs were treated with the agonists $C_4.T_4$ (C_4/TDB: 24 μg/ml, T_4/ultra-pure LPS: 10 ng/ml) for 16 h and 48 h, respectively, in 48 well plate. Where indicated, INH (isoniazid) (2.5 μg/ml) and RIF (rifampicin) (0.5 μg/ml) were incubated along with the $C_4.T_4$ agonists.

Determination of CFUs

Intracellular *Mtb* growth in BMDMs and THP-1 macrophages were enumerated after 4 h of *Mtb* infection followed by 48 h of stimulation with $C_4.T_4$. The cell SNs were collected for ELISA and 0.1% saponin (in water) was added to lyse the cells, followed by 10-fold serial dilutions and plating on 7H11 agar to enumerate CFUs. The colonies were counted 3 days (*M. smegmatis*) and 3 wks (H37Rv and H37Ra) after incubation at 37°C (5% CO_2).

Nitric oxide (NO) production

Culture SNs of *Mtb*-infected BMDMs or lung cells from *Mtb*-infected mice were harvested after 48 h and NO was measured by the Griess method. In brief, SNs were added to an equal volume (50 μl) of Griess reagent for 5 min at RT and absorbance at 550 nm was assessed. The measurement of NO was performed by comparing with sodium nitrite ($NaNO_2$) as a standard (μM).

Antigen uptake

BMDMs (2.5×10^5/well) were stimulated in either the presence or the absence of CLEC4E/C_4 (24 μg/ml) and TLR4/T_4 (10 ng/ml) agonists for 48 h. The cells were then infected with GFP-*Mtb* (H37Ra) at MOI 1:3 for 4 h. BMDMs were washed vigorously (3 X) with ice cold PBS. The cells were then treated with amikacin (2 μg/ml) and incubated for 1h to remove extracellular *Mtb* and fixed with paraformaldehyde (1%). The cells were washed and placed on poly-L-lysine coated coverslips and imaged using confocal microscopy (Nikon A1; Nikon, Tokyo, Japan). Z-stacks were taken to exclude the interference of extracellular bacteria. Analysis was performed using Nikon NIS-AR 4.1 image analysis software (Nikon, Melville, NY). Further, the confocal results were authenticated by flow cytometry. The analysis was done by FACS Suite software (BD Biosciences, San Jose, CA).

The enumeration of bacterial uptake was done through CFUs. BMDMs (2.5×10^5/well) were stimulated with CLEC4E/C_4 (24 μg/ml) and TLR4/T_4 (10 ng/ml) agonists for 48 h. BMDMs were harvested and infected with H37Rv at MOI (1:5) for 4 h. The cells were then treated with amikacin (2 μg/ml) and incubated for 1 h to remove extracellular *Mtb*. Later, the cells were lysed with saponin (0.1% in water) and subsequent plating was performed with 10-fold serial dilutions on 7H11 plates. The colonies were counted 3 weeks after incubation at 37°C (5% CO_2).

Western blot

Mtb-(H37Rv and H37Ra) infected BMDMs (2.5 X 10^6 cells/well) were treated with CLEC4E/C_4 (24 μg/ml) and TLR4/T_4 (10 ng/ml) agonists for 15–30 min (STAT1, STAT6, PtdIns3K), 1 h (MYD88, Phospho MTOR), 4 h (LC3B, SQSTM1), 18 h (NOS2), and 24 h (BCL2L1) in 12 well plates. The cells were then harvested, washed and lysed in cytosolic extraction lysis buffer (with PMSF, protease and phosphatase inhibitor cocktail). Cytosolic protein was then quantified and subjected to SDS-PAGE electrophoresis. After transfer to PVDF membranes and following blocking with BSA (2%), the membranes were immunoblotted with phosphorylated and non-phosphorylated Abs against STAT1, STAT6, PtdIns3K, MYD88, MTOR, LC3B, NOS2, BCL2L1. ACTB was used as a loading control. Regular washing was performed in each step. Blots were developed using a chemiluminescence kit (Amersham Pharmacia Biotech, Buckinghamshire, UK and ECL; Pharmacia-Amersham, Freiburg, Germany). Scanning of the blots was completed with ImageQuant LAS 4000 (GE Healthcare, Pittsburgh, PA). The image analysis was achieved with MultiGuage and ImageJ analysis software. Cells stimulated with LPS (2 μg/ml) were used as a positive control.

Expression of LC3, LAMP1, RELA/NFKB p65 by confocal microscopy

BMDMs were placed on poly-L-lysine pre-coated coverslips for 3 h. The cells were stimulated with $C_4.T_4$ for 4 h (LC3), 8–10 h (LAMP1) and 30 min (RELA/NFKB p65). The cells were fixed with 2% PFA (paraformaldehyde) for 10 min. This was

followed by treatment with Triton X-100 (0.1%) for 2 min. To block non-specific binding, macrophages were incubated with BSA (2%) for 2 h, followed by addition of primary Abs for 2 h. Afterward, cells were incubated with secondary Ab for 1 h. The cells were stained with DAPI for 10 min at RT. Cells were washed in between each step. The cells on coverslips were mounted onto slides with Fluoromount-G. The cells were imaged using confocal (NIKON A1) microscopy (Nikon, Tokyo, Japan). Analysis was achieved by Nikon-NIS-AR 4.1 image analysis software (Nikon, Melville, NY). Positive controls for LC3 and RELA/NFKB p65 labeling involved starving macrophages in HBSS medium and LPS, respectively. For co-localization of *Mtb* with autophagosomes (LC3) and lysosomes (LAMP1), BMDMs were infected with GFP-*Mtb* for 4 h, followed by stimulation with $C_4.T_4$. Cells having 5 or more LC3 puncta were recorded as LC3-positive cells. The formation of LC3 puncta was manually counted in at least 50 cells for each group and plotted as number of puncta per cells with fluorescent LC3 puncta.

Acridine orange, MDC and LysoTracker Red staining

BMDMs were treated with the autophagy inhibitor 3MA (10 mM) for 1 h, prior to $C_4.T_4$ stimulation for 4 h (acridine orange and MDC staining), followed by incubation at 37°C with acridine orange (1 μg/ml) or 0.05 mM MDC for 20 min. The cells were fixed with 2% PFA at RT and observed immediately with an immunofluorescence microscope (Olympus IX71/TH4 200, Hamburg, Germany). For LysoTracker Red staining, BMDMs were infected with GFP-*Mtb* for 4 h and treated with $C_4.T_4$ for 8–10 h. The cells were then fixed with PFA (2%) for 10 min and treated with Triton X-100 (0.1%) for 2 min. The cells were stained with 100 nM LysoTracker Red for 30 min at 37°C and then observed either through confocal microscope (Nikon A1R, Nikon, Yokohama, Japan) or flow cytometer (BD FACS ARIA, BD Biosciences, CA). For flow cytometry experiments, the BMDMs were treated with 3MA for 1 h prior $C_4.T_4$ stimulation.

Demonstration of RELA/NFKB by EMSA

BMDMs were washed and treated with CLEC4E/C_4 (24 μg/ml) and TLR4/T_4 (10 ng/ml) for 30 min. The cells were then harvested, and the nuclear extract was collected. EMSA was performed after P^{32} probe labeling. In brief, an equal concentration of nuclear protein (3 μg) from each sample was incubated for 20 min at 37°C in a water bath with [P^{32}] end labeled duplex oligonucleotides that contain the binding site for RELA/NFKB. The DNA–protein complexes were resolved on a native PAGE-gel (7%) by electrophoresis. The gel was dried at 80°C in a vacuum gel dryer for 2 h and exposed to screen at RT for 6–12 h and scanned by phosphor-imager scanning screen (Fujifilm, FLA-5000, Tokyo, Japan).

RELA/NFKB nuclear translocation by confocal microscopy

BMDMs were placed on poly-L-lysine pre-coated coverslips for 2 h. The cells were then stimulated with $C_4.T_4$ for 30 min at 37°C. Cells were then fixed with PFA (2%) for 5–10 min, followed by treatment with Triton X-100 (0.1%) for 2 min. The samples were incubated with BSA (2%) to block the non-specific sites for 2 h. The cells were then incubated with anti-mouse RELA/NFKB p65 Ab (1:400) for 2 h. Afterward, cells were treated with Alexa fluor 633-anti-rabbit Ab for 1 h and then stained with DAPI for 10 min. Regular washings with 1XPBS were conducted at each step. The samples were mounted on slides with Fluoromount-G and cells were imaged with a Nikon A1 confocal laser microscope (Nikon, Tokyo, Japan). The data were analyzed using image analysis software Nikon NIS-AR 4.1 (Nikon, Melville, NY).

The quantification of autophagy-related genes by real time PCR

Total RNA was isolated from the lungs of mice immunized with $C_4.T_4$ using trizol reagent, according to the manufacturer's instruction (Invitrogen, Carlsbad, CA). RNA was quantified through NanoDrop machine (BioTek, Winooski, VT). Purity of all RNA samples was measured by A260/A280 ratio and was in the range of 1.9 to 2.0. All RNA samples (3 μg) were treated with amplification grade DNase 1 (3 U) (Sigma Aldrich, AMPD1-1KT) for 15 min in 1 X reaction buffer to avoid DNA contamination. DNase activity was stopped with stop solution (Sigma Aldrich, AMPD1-1KT) and then incubating the samples at 70°C for 10 min. The cDNA was then prepared by maxima first strand cDNA synthesis kit for RT-qPCR (Thermo Fisher Scientific, K1642). Real time PCR and data analysis was done by the ABI 7500 Fast Real-time PCR system (Applied Biosystems, Chromos, Singapore), with ACTB as a loading control. Analysis was done by the comparative Ct method. Results are presented as relative expression (fold change). The primer sequences for RT-qPCR are in Figure S15.

siRNA transfection of Becn1 in BMDMs

BMDMs were cultured in 48 well plate and transient knockdown of *Becn1*, 120 nM of FlexiTube siRNA GeneSolution (Qiagen, GS56208), comprising of 4 different target sequences or a scrambled siRNA control were taken to transfect 2.5×10^5 cells, as per manufacturer's instructions. After 72 h, the cells were infected with *Mtb*-H37Rv (MOI 1:5) and harvested after 4 h. The extracellular bacteria were removed by treating cultures with amikacin (2 μg/ml) followed by extensive washing with PBS. Then *Mtb*-infected BMDMs were treated with the $C_4.T_4$ agonists (C_4/TDB: 24 μg/ml, T_4/ultra-pure LPS: 10 ng/ml) for 8 h (RT-qPCR) and 48 h (CFU assay).

Treatment of Mtb-infected mice with $C_4.T_4$

Mice (100 CFUs) and guinea pigs (30 CFUs) were aerosol challenged with *Mtb* and then treated with $C_4.T_4$ in the footpad for a total of 2 injections with an interval of 10 d. The control groups were treated with either CLEC4E (50 μg/100 μl/mouse; 200 μg/200 μl/guinea pig) or TLR4 (0.1 μg/100 μl/mouse; 1 μg/200 μl/guinea pig) agonists or PBS. Anti-TB drugs (rifampicin: 0.5, 1, 10 mg/kg bw of mice; 6 mg/kg

bw guinea pig and isoniazid: 5 mg/kg bw of guinea pig) were orally administrated twice with 0.1% CMC (carboxymethylcellulose) (Sigma Aldrich, C5013). After 45 d of aerosol challenge, animals were sacrificed, and then bacterial burden was enumerated in the lung, liver and spleen by CFUs. CFUs were calculated taking into consideration weight of the organs.

Isolation of T lymphocytes, enumeration of cell surface and intracellular expression

Mice were aerosol challenged with *Mtb*. After 21 d, experimental groups were administered $C_4.T_4$ and controls with PBS twice at an interval of 10 d. Forty-five days later, animals were sacrificed. The mice and guinea pigs were perfused with PBS-heparin and spleen, lymph nodes (mediastinal) and lungs were harvested, and then single cell suspensions were made. Briefly, RBCs were removed with ACK (NH_4Cl, 0.15 M, $KHCO_3$ 10 mM, EDTA 88 mM) lysis buffer, washed 3X with PBS and lymphocytes isolated from spleen and lungs were re-suspended in RPMI-1640-FBS-10%. Cell viability was measured by trypan blue dye exclusion. *In vitro* experiments were conducted in the presence of purified protein derivative (PPD) to detect intracellular expression of cytokines and frequency of effector/central memory populations in *Mtb*-specific T cells.

Histopathology

Mice and guinea pigs were sacrificed, and lung and spleen tissues were fixed in buffered formalin (10%). Histological sections were stained using hematoxylin and eosin. The microscopic photographs were taken using an Olympus IX71 microscope and displayed at 10X and 40X magnifications.

Statistical analysis

Analysis of all data was done by Student's "t" test, non-parametric Mann-Whitney two tailed and repeated measure ANOVA with post Student-Newman-Keuls multiple comparison test using Graph Pad InStat 3 and Graph Pad Prism 6 software. The statistical differences were considered significant at a level of $p < 0.05$.

Acknowledgments

We are thankful to Prof. B. N. Datta (Medicos Center, Chandigarh, India) for the analysis of histopathology sections, Council of Scientific & Industrial Research (CSIR) for financial support. SP was the recipient of the fellowship of CSIR; SN from Department of Biotechnology (DBT); MA from Department of Science and Technology (DST). We appreciate Dr. Chrissy Leopold Wager (Texas Biomedical Research Institute, Texas, USA), and Dr. Ansu Louis, Dr. Gurpreet Kaur (Indian Institute of Technology, Ropar, India) for critically evaluating the manuscript.

Disclosure statement

No potential conflict of interest was reported by the authors.

Funding

We thank the Council of Scientific & Industrial Research (CSIR) for financial support (Project Number: OLP 088).

References

[1] World Health Organization (WHO). Global tuberculosis report 2017. Geneva: WHO; 2017. [cited 2017 Nov 14]. Available from http://www.who.int/tb/publications/global_report/en/

[2] World Health Organization (WHO). Global tuberculosis report. Geneva: World Health Organization; 2018. Available from http://www.who.int/iris/handle/10665/274453

[3] Lawn SD, Zumla AI. Tuberculosis. Lancet. 2011 Jul 02;378(9785):57–72. PubMed PMID: 21420161.

[4] Prabowo SA, Groschel MI, Schmidt ED, et al. Targeting multidrug-resistant tuberculosis (MDR-TB) by therapeutic vaccines. Med Microbiol Immunol. 2013 Apr;202(2):95–104. PubMed PMID: 23143437.

[5] Kaufmann SH. Tuberculosis vaccines: time to think about the next generation. Semin Immunol. 2013 Apr;25(2):172–181. PubMed PMID: 23706597.

[6] Howitt MR, Garrett WS. A complex microworld in the gut: gut microbiota and cardiovascular disease connectivity. Nat Med. 2012 Aug;18(8):1188–1189. PubMed PMID: 22869188.

[7] Mukaida N. Intestinal microbiota: unexpected alliance with tumor therapy. Immunotherapy. 2014;63:231–233. PubMed PMID: 24762069

[8] Pyonteck SM, Akkari L, Schuhmacher AJ, et al. CSF-1R inhibition alters macrophage polarization and blocks glioma progression. Nat Med. 2013 Oct;19(10):1264–1272. PubMed PMID: 24056773.

[9] Organization WH. WHO report 2007: global tuberculosis control: surveillance, planning, financing. Geneva: World health organization; 2007.

[10] Pahari S, Kaur G, Aqdas M, et al. Bolstering immunity through pattern recognition receptors: a unique approach to control tuberculosis. Front Immunol. 2017;8:906. PubMed PMID: 28824632.

[11] Schoenen H, Bodendorfer B, Hitchens K, et al. Cutting edge: mincle is essential for recognition and adjuvanticity of the mycobacterial cord factor and its synthetic analog trehalose-dibehenate. J Immunol. 2010 Mar 15;184(6):2756–2760. PubMed PMID: 20164423.

[12] Yamasaki S, Ishikawa E, Sakuma M, et al. Mincle is an ITAM-coupled activating receptor that senses damaged cells. Nat Immunol. 2008 Oct;9(10):1179–1188. PubMed PMID: 18776906.

[13] Suzuki Y, Nakano Y, Mishiro K, et al. Involvement of mincle and syk in the changes to innate immunity after ischemic stroke. Sci Rep. 2013 Nov 11;3:3177. PubMed PMID: 24212132.

[14] de Rivero Vaccari JC, Brand FJ 3rd, Berti AF, et al. Mincle signaling in the innate immune response after traumatic brain injury. J Neurotrauma. 2015 Feb 15;32(4):228–236. PubMed PMID: 25111533.

[15] Wells CA, Salvage-Jones JA, Li X, et al. The macrophage-inducible C-type lectin, mincle, is an essential component of the innate immune response to *Candida albicans*. J Immunol. 2008 Jun 1;180(11):7404–7413. PubMed PMID: 18490740.

[16] Bugarcic A, Hitchens K, Beckhouse AG, et al. Human and mouse macrophage-inducible C-type lectin (Mincle) bind *Candida albicans*. Glycobiology. 2008 Sep;18(9):679–685. PubMed PMID: 18509109.

[17] Vijayan D, Radford KJ, Beckhouse AG, et al. Mincle polarizes human monocyte and neutrophil responses to *Candida albicans*. Immunol Cell Biol. 2012 Oct;90(9):889–895. PubMed PMID: 22641025.

[18] Yamasaki S, Matsumoto M, Takeuchi O, et al. C-type lectin Mincle is an activating receptor for pathogenic fungus, Malassezia. Proc Natl Acad Sci U S A. 2009 Feb 10;106(6):1897–1902. PubMed PMID: 19171887.

[19] Ishikawa T, Itoh F, Yoshida S, et al. Identification of distinct ligands for the C-type lectin receptors Mincle and Dectin-2 in the pathogenic fungus Malassezia. Cell Host Microbe. 2013 Apr 17;13(4):477–488. PubMed PMID: 23601109.
[20] Wevers BA, Kaptein TM, Zijlstra-Willems EM, et al. Fungal engagement of the C-type lectin mincle suppresses Dectin-1-induced antifungal immunity. Cell Host Microbe. 2014 Apr 09;15(4):494–505. PubMed PMID: 24721577.
[21] Bekierkunst A, Yarkoni E, Flechner I, et al. Immune response to sheep red blood cells in mice pretreated with mycobacterial fractions. Infect Immun. 1971 Sep;4(3):256–263. PubMed PMID: 4949490.
[22] Geisel RE, Sakamoto K, Russell DG, et al. *In vivo* activity of released cell wall lipids of *Mycobacterium bovis* bacillus Calmette-Guerin is due principally to trehalose mycolates. J Immunol. 2005 Apr 15;174(8):5007–5015. PubMed PMID: 15814731.
[23] van Dissel JT, Joosten SA, Hoff ST, et al. A novel liposomal adjuvant system, CAF01, promotes long-lived *Mycobacterium tuberculosis*-specific T-cell responses in human. Vaccine. 2014 Dec 12;32(52):7098–7107. PubMed PMID: 25454872.
[24] Agger EM, Rosenkrands I, Hansen J, et al. Cationic liposomes formulated with synthetic mycobacterial cordfactor (CAF01): a versatile adjuvant for vaccines with different immunological requirements. PLoS One. 2008 Sep 08;3(9):e3116. PubMed PMID: 18776936.
[25] Pimm MV, Baldwin RW, Polonsky J, et al. Immunotherapy of an ascitic rat hepatoma with cord factor (trehalose-6, 6′-dimycolate) and synthetic analogues. Int J Cancer. 1979 Dec 15;24(6):780–785. PubMed PMID: 544531.
[26] Olds GR, Chedid L, Lederer E, et al. Induction of resistance to Schistosoma mansoni by natural cord factor and synthetic lower homologues. J Infect Dis. 1980 Apr;141(4):473–478. PubMed PMID: 7373082.
[27] Davidsen J, Rosenkrands I, Christensen D, et al. Characterization of cationic liposomes based on dimethyldioctadecylammonium and synthetic cord factor from *M. tuberculosis* (trehalose 6,6′-dibehenate)-a novel adjuvant inducing both strong CMI and antibody responses. Biochim Biophys Acta. 2005 Dec 10;1718(1–2):22–31. PubMed PMID: 16321607.
[28] Pasare C, Medzhitov R. Toll-like receptors: linking innate and adaptive immunity. Microbes Infect. 2004 Dec;6(15):1382–1387. . PubMed PMID: 15596124.
[29] Hemmi H, Akira S. TLR signalling and the function of dendritic cells. Chem Immunol Allergy. 2005;86:120–135. PubMed PMID: 15976491.
[30] Holscher C, Reiling N, Schaible UE, et al. Containment of aerogenic *Mycobacterium tuberculosis* infection in mice does not require MyD88 adaptor function for TLR2, −4 and −9. Eur J Immunol. 2008 Mar;38(3):680–694. PubMed PMID: 18266299.
[31] Vacchelli E, Galluzzi L, Eggermont A, et al. Trial watch: FDA-approved toll-like receptor agonists for cancer therapy. Oncoimmunology. 2012 Sep 1;1(6):894–907. PubMed PMID: 23162757.
[32] Needham BD, Carroll SM, Giles DK, et al. Modulating the innate immune response by combinatorial engineering of endotoxin. Proc Natl Acad Sci U S A. 2013 Jan 22;110(4):1464–1469. PubMed PMID: 23297218.
[33] Bohannon JK, Hernandez A, Enkhbaatar P, et al. The immunobiology of toll-like receptor 4 agonists: from endotoxin tolerance to immunoadjuvants. Shock. 2013 Dec;40(6):451–462. PubMed PMID: 23989337.
[34] Gantner BN, Simmons RM, Canavera SJ, et al. Collaborative induction of inflammatory responses by dectin-1 and toll-like receptor 2. J Exp Med. 2003 May 05;197(9):1107–1117. PubMed PMID: 12719479.
[35] Loures FV, Araujo EF, Feriotti C, et al. TLR-4 cooperates with Dectin-1 and mannose receptor to expand Th17 and Tc17 cells induced by Paracoccidioides brasiliensis stimulated dendritic cells. Front Microbiol. 2015;6:261. PubMed PMID: 25873917.
[36] Gutierrez MG, Master SS, Singh SB, et al. Autophagy is a defense mechanism inhibiting BCG and *Mycobacterium tuberculosis* survival in infected macrophages. Cell. 2004 Dec 17;119(6):753–766. PubMed PMID: 15607973.
[37] Castillo EF, Dekonenko A, Arko-Mensah J, et al. Autophagy protects against active tuberculosis by suppressing bacterial burden and inflammation. Proc Natl Acad Sci U S A. 2012 Nov 13;109(46):E3168–76. PubMed PMID: 23093667.
[38] Klein L, Munz C, Lunemann JD. Autophagy-mediated antigen processing in CD4(+) T cell tolerance and immunity. FEBS Lett. 2010 Apr 02;584(7):1405–1410. PubMed PMID: 20074571.
[39] Lunemann JD, Munz C. Autophagy in CD4+ T-cell immunity and tolerance. Cell Death Differ. 2009 Jan;16(1):79–86. . PubMed PMID: 18636073.
[40] Xu Y, Jagannath C, Liu XD, et al. Toll-like receptor 4 is a sensor for autophagy associated with innate immunity. Immunity. 2007 Jul;27(1):135–144. PubMed PMID: 17658277.
[41] Shi CS, Kehrl JH. MyD88 and trif target Beclin 1 to trigger autophagy in macrophages. J Biol Chem. 2008 Nov 28;283(48):33175–33182. . PubMed PMID: 18772134.
[42] Medzhitov R. Recognition of microorganisms and activation of the immune response. Nature. 2007 Oct 18;449(7164):819–826. . PubMed PMID: 17943118.
[43] LeibundGut-Landmann S, Gross O, Robinson MJ, et al. Syk- and CARD9-dependent coupling of innate immunity to the induction of T helper cells that produce interleukin 17. Nat Immunol. 2007 Jun;8(6):630–638. PubMed PMID: 17450144.
[44] Ostrop J, Jozefowski K, Zimmermann S, et al. Contribution of MINCLE-SYK signaling to activation of primary human APCs by mycobacterial cord factor and the novel adjuvant TDB. J Immunol. 2015 Sep 01;195(5):2417–2428. PubMed PMID: 26202982.
[45] Domingo-Gonzalez R, Prince O, Cooper A, et al. Cytokines and chemokines in *Mycobacterium tuberculosis* infection. Microbiol Spectr. 2016 Oct;4(5). PubMed PMID: 27763255. DOI:10.1128/microbiolspec.TBTB2-0018-2016.
[46] Stockinger B. Capacity of antigen uptake by B cells, fibroblasts or macrophages determines efficiency of presentation of a soluble self antigen (C5) to T lymphocytes. Eur J Immunol. 1992 May;22(5):1271–1278. PubMed PMID: 1577067.
[47] Pahari S, Khan N, Aqdas M, et al. Infergen stimulated macrophages restrict *Mycobacterium tuberculosis* growth by autophagy and release of nitric oxide. Sci Rep. 2016 Dec 21;6:39492. PubMed PMID: 28000752.
[48] Khan N, Pahari S, Vidyarthi A, et al. Stimulation through CD40 and TLR-4 is an effective host directed therapy against *Mycobacterium tuberculosis*. Front Immunol. 2016;7:386. PubMed PMID: 27729911.
[49] Khan N, Pahari S, Vidyarthi A, et al. NOD-2 and TLR-4 signaling reinforces the efficacy of dendritic cells and reduces the dose of tb drugs against *Mycobacterium tuberculosis*. J Innate Immun. 2016;8(3):228–242. PubMed PMID: 26613532.
[50] Quenelle DC, Staas JK, Winchester GA, et al. Efficacy of microencapsulated rifampin in *Mycobacterium tuberculosis*-infected mice. Antimicrob Agents Chemother. 1999 May;43(5):1144–1151. PubMed PMID: 10223927.
[51] Flynn JL, Chan J, Triebold KJ, et al. An essential role for interferon gamma in resistance to *Mycobacterium tuberculosis* infection. J Exp Med. 1993 Dec 01;178(6):2249–2254. PubMed PMID: 7504064.
[52] Monin L, Griffiths KL, Slight S, et al. Immune requirements for protective Th17 recall responses to *Mycobacterium tuberculosis* challenge. Mucosal Immunol. 2015 Sep;8(5):1099–1109. PubMed PMID: 25627812.
[53] Caccamo N, Guggino G, Joosten SA, et al. Multifunctional CD4(+) T cells correlate with active *Mycobacterium tuberculosis* infection. Eur J Immunol. 2010 Aug;40(8):2211–2220. PubMed PMID: 20540114.
[54] Rai PK, Chodisetti SB, Nadeem S, et al. A novel therapeutic strategy of lipidated promiscuous peptide against *Mycobacterium*

tuberculosis by eliciting Th1 and Th17 immunity of host. Sci Rep. 2016 Apr 07;6:23917. PubMed PMID: 27052185.

[55] Forbes EK, Sander C, Ronan EO, et al. Multifunctional, high-level cytokine-producing Th1 cells in the lung, but not spleen, correlate with protection against *Mycobacterium tuberculosis* aerosol challenge in mice. J Immunol. 2008 Oct 01;181(7):4955–4964. PubMed PMID: 18802099.

[56] Ni Cheallaigh C, Keane J, Lavelle EC, et al. Autophagy in the immune response to tuberculosis: clinical perspectives. Clin Exp Immunol. 2011 Jun;164(3):291–300. PubMed PMID: 21438870.

[57] Khader SA, Bell GK, Pearl JE, et al. IL-23 and IL-17 in the establishment of protective pulmonary CD4+ T cell responses after vaccination and during *Mycobacterium tuberculosis* challenge. Nat Immunol. 2007 Apr;8(4):369–377. PubMed PMID: 17351619.

[58] Riol-Blanco L, Sanchez-Sanchez N, Torres A, et al. The chemokine receptor CCR7 activates in dendritic cells two signaling modules that independently regulate chemotaxis and migratory speed. J Immunol. 2005 Apr 1;174(7):4070–4080. PubMed PMID: 15778365.

[59] Seth S, Oberdorfer L, Hyde R, et al. CCR7 essentially contributes to the homing of plasmacytoid dendritic cells to lymph nodes under steady-state as well as inflammatory conditions. J Immunol. 2011 Mar 15;186(6):3364–3372. PubMed PMID: 21296980.

[60] Jo EK. Innate immunity to mycobacteria: vitamin D and autophagy. Cell Microbiol. 2010 Aug;12(8):1026–1035. PubMed PMID: 20557314.

[61] Khan N, Vidyarthi A, Pahari S, et al. Signaling through NOD-2 and TLR-4 bolsters the T cell priming capability of dendritic cells by inducing autophagy. Sci Rep. 2016 Jan 12;6:19084. PubMed PMID: 26754352.

[62] Harris J, De Haro SA, Master SS, et al. T helper 2 cytokines inhibit autophagic control of intracellular *Mycobacterium tuberculosis*. Immunity. 2007 Sep;27(3):505–517. PubMed PMID: 17892853.

[63] Vergne I, Singh S, Roberts E, et al. Autophagy in immune defense against *Mycobacterium tuberculosis*. Autophagy. 2006 Jul–Sep;2(3):175–178. PubMed PMID: 16874111.

[64] Barth S, Glick D, Macleod KF. Autophagy: assays and artifacts. J Pathol. 2010 Jun;221(2):117–124. PubMed PMID: 20225337.

[65] Cemma M, Brumell JH. Interactions of pathogenic bacteria with autophagy systems. Curr Biol. 2012 Jul 10;22(13):R540–5. PubMed PMID: 22790007.

[66] Tapper H, Sundler R. Bafilomycin A1 inhibits lysosomal, phagosomal, and plasma membrane H(+)-ATPase and induces lysosomal enzyme secretion in macrophages. J Cell Physiol. 1995 Apr;163(1):137–144. PubMed PMID: 7896890.

[67] Drose S, Altendorf K. Bafilomycins and concanamycins as inhibitors of V-ATPases and P-ATPases. J Exp Biol. 1997 Jan;200(Pt 1):1–8. PubMed PMID: 9023991.

[68] Desel C, Werninghaus K, Ritter M, et al. The Mincle-activating adjuvant TDB induces MyD88-dependent Th1 and Th17 responses through IL-1R signaling. PLoS One. 2013;8(1):e53531. PubMed PMID: 23308247.

[69] Kleinnijenhuis J, Oosting M, Joosten LA, et al. Innate immune recognition of *Mycobacterium tuberculosis*. Clin Dev Immunol. 2011;2011:405310. PubMed PMID: 21603213.

[70] Zhou ZQ, Wang ZK, Zhang L, et al. Role of EAST-6 in renal injury by regulating microRNA-155 expression via TLR4/MyD88 signaling pathway in mice with *Mycobacterium tuberculosis* infection. Biosci Rep. 2017 Jun 27 PubMed PMID: 28655852. DOI:10.1042/BSR20170021

[71] Paglin S, Hollister T, Delohery T, et al. A novel response of cancer cells to radiation involves autophagy and formation of acidic vesicles. Cancer Res. 2001 Jan 15;61(2):439–444. PubMed PMID: 11212227.

[72] Brungs S, Kolanus W, Hemmersbach R. Syk phosphorylation - a gravisensitive step in macrophage signalling. Cell Commun Signal. 2015 Feb 03;13:9.

[73] Zhang J, Wang X, Vikash V, et al. ROS and ROS-Mediated Cellular Signaling. Oxid Med Cell Longev. 2016;2016:4350965. PubMed PMID: 26998193.

[74] Nakajima S, Kitamura M. Bidirectional regulation of NF-kappaB by reactive oxygen species: a role of unfolded protein response. Free Radic Biol Med. 2013 Dec;65:162–174. PubMed PMID: 23792277.

[75] Chan J, Tanaka K, Carroll D, et al. Effects of nitric oxide synthase inhibitors on murine infection with *Mycobacterium tuberculosis*. Infect Immun. 1995;63(2):736–740.

[76] Chan J, Xing Y, Magliozzo RS, et al. Killing of virulent *Mycobacterium tuberculosis* by reactive nitrogen intermediates produced by activated murine macrophages. J Exp Med. 1992;175(4):1111–1122.

[77] Abel B, Thieblemont N, Quesniaux VJ, et al. Toll-like receptor 4 expression is required to control chronic *Mycobacterium tuberculosis* infection in mice. J Immunol. 2002 Sep 15;169(6):3155–3162. PubMed PMID: 12218133.

[78] Miyake Y, Toyonaga K, Mori D, et al. C-type lectin MCL is an FcRgamma-coupled receptor that mediates the adjuvanticity of mycobacterial cord factor. Immunity. 2013 May 23;38(5):1050–1062. PubMed PMID: 23602766.

[79] Ishikawa E, Ishikawa T, Morita YS, et al. Direct recognition of the mycobacterial glycolipid, trehalose dimycolate, by C-type lectin Mincle. J Exp Med. 2009 Dec 21;206(13):2879–2888. PubMed PMID: 20008526.

[80] Arnett E, Krishnan N, BD R, et al. Host pathogen biology for airborne *Mycobacterium tuberculosis*. In: Hickey A, Misra A, Fourie Peditors. Drug delivery systems for tuberculosis preveniton and treatment. Cellular and molecular events in the lung. Chichester, UK: John Wiley & Sons, Ltd; 2016. p. 11–47.

[81] Paunescu E. In vivo and in vitro suppression of humoral and cellular immunological response by rifampicin. Nature. 1970 Dec 19;228(5277):1188–1190. PubMed PMID: 5487244.

[82] Bellahsene A, Forsgren A. Effect of rifampin on the immune response in mice. Infect Immun. 1980 Jan;27(1):15–20. PubMed PMID: 6987166; PubMed Central PMCID: PMCPMC550714.

[83] Floersheim GL. Suppression of cellular immunity in vivo by rifampicin. Experientia. 1973 Dec;29(12):1545–1546. PubMed PMID: 4589325.

[84] Manabe YC, Bishai WR. Latent *Mycobacterium tuberculosis*-persistence, patience, and winning by waiting. Nat Med. 2000 Dec;6(12):1327–1329. . PubMed PMID: 11100115.

[85] Canaday DH, Wilkinson RJ, Li Q, et al. CD4(+) and CD8(+) T cells kill intracellular *Mycobacterium tuberculosis* by a perforin and Fas/Fas ligand-independent mechanism. J Immunol. 2001 Sep 01;167(5):2734–2742. PubMed PMID: 11509617.

[86] He XY, Xiao L, Chen HB, et al. T regulatory cells and Th1/Th2 cytokines in peripheral blood from tuberculosis patients. Eur J Clin Microbiol Infect Dis. 2010 Jun;29(6):643–650. PubMed PMID: 20306324.

[87] Singh V, Gowthaman U, Jain S, et al. Coadministration of interleukins 7 and 15 with bacille Calmette-Guerin mounts enduring T cell memory response against *Mycobacterium tuberculosis*. J Infect Dis. 2010 Aug 15;202(3):480–489. PubMed PMID: 20569158.

[88] Lindenstrom T, Agger EM, Korsholm KS, et al. Tuberculosis subunit vaccination provides long-term protective immunity characterized by multifunctional CD4 memory T cells. J Immunol. 2009 Jun 15;182(12):8047–8055. PubMed PMID: 19494330.

[89] Pahari S, Kaur G, Negi S, et al. Reinforcing the functionality of mononuclear phagocyte system to control tuberculosis. Front Immunol. 2018;9:193. PubMed PMID: 29479353.

[90] Deretic V. Autophagy in tuberculosis. Cold Spring Harb Perspect Med. 2014 Aug 28;4(11):a018481. . PubMed PMID: 25167980.

[91] Watson RO, Manzanillo PS, Cox JS. Extracellular *M. tuberculosis* DNA targets bacteria for autophagy by activating the host DNA-sensing pathway. Cell. 2012 Aug 17;150(4):803–815. . PubMed PMID: 22901810.

[92] Seto S, Tsujimura K, Horii T, et al. Autophagy adaptor protein p62/SQSTM1 and autophagy-related gene Atg5 mediate autophagosome

formation in response to *Mycobacterium tuberculosis* infection in dendritic cells. PLoS One. 2013;8(12):e86017. PubMed PMID: 24376899.

[93] Franco LH, Nair VR, Scharn CR, et al. The ubiquitin ligase smurf1 functions in selective autophagy of *Mycobacterium tuberculosis* and anti-tuberculous host defense. Cell Host Microbe. 2017 Jan 11;21(1):59–72. PubMed PMID: 28017659.

[94] Kimmey JM, Huynh JP, Weiss LA, et al. Unique role for ATG5 in neutrophil-mediated immunopathology during *M. tuberculosis* infection. Nature. 2015 Dec 24;528(7583):565–569. PubMed PMID: 26649827; PubMed Central PMCID: PMCPMC4842313.

[95] Behar SM, Baehrecke EH. Tuberculosis: autophagy is not the answer. Nature. 2015 Dec 24;528(7583):482–483. . PubMed PMID: 26649822.

[96] Dallenga T, Repnik U, Corleis B, et al. *M. tuberculosis*-induced necrosis of infected neutrophils promotes bacterial growth following phagocytosis by macrophages. Cell Host Microbe. 2017 Oct 11;22(4):519–530 e3. PubMed PMID: 29024644.

[97] Jagannath C, Lindsey DR, Dhandayuthapani S, et al. Autophagy enhances the efficacy of BCG vaccine by increasing peptide presentation in mouse dendritic cells. Nat Med. 2009 Mar;15 (3):267–276. PubMed PMID: 19252503.